

Design Parameter Analysis of a Single-Effect Solar Still

A project report

submitted by

SEETHARAMAN SUBRAMANIAN

in partial fulfilment of the requirements

for the award of the degree of

**BACHELOR OF TECHNOLOGY IN
ENGINEERING DESIGN
AND
MASTER OF TECHNOLOGY IN
AUTOMOTIVE ENGINEERING**



**DEPARTMENT OF ENGINEERING DESIGN
INDIAN INSTITUTE OF TECHNOLOGY MADRAS.**

May 2019

CERTIFICATE

This is to certify that the project titled **Design Parameter Analysis of a Single-Effect Solar Still**, submitted by **Mr Seetharaman Subramanian**, to the Indian Institute of Technology Madras, for the award of the degrees of **Bachelor of Technology** and **Master of Technology**, is a *bona fide* record of the research work done by him under my supervision. The contents of this project, in full or in parts, have not been submitted to any other Institute or University for the award of any degree or diploma.

Dr Sandipan Bandyopadhyay
Project Adviser
Associate Professor
Department of Engineering Design
Indian Institute of Technology Madras
Chennai 600 036

Place: Chennai

Date: May 6, 2019

ACKNOWLEDGEMENTS

I want to thank my guide, Dr Sandipan Bandyopadhyay for providing his perspective on this topic and guiding me in this project. I would also like to thank Mr Amey Pednekar, upon whose shoulders this project stands, and all the professors whose teachings have made me into the engineer that I am today. I would also like to extend my gratitude towards my friends Mr Shashwat Joshi and Mr Akhil Sathuluri, without whose guidance and help I would not have been able to build my prototypes. I would, lastly, like to thank the reader as well for showing the patience to read through my report.

ABSTRACT

KEYWORDS: Solar energy, solar still, inclined-basin solar still

A solar still is no different in theory now than the ones built hundreds of years ago. What has changed has the understanding of the design parameters that have an impact on the performance of the still. This work aims at understanding the theory behind the thermodynamics of the still, and how it leads to the various design parameters and the extent of the impact of these parameters on the performance of the still.

The design of an inclined-basin solar still is proposed, wherein the floor of the basin is also inclined to increase the amount of incident solar energy. Effects of variations in the design parameters on the performance and output of the still are observed. The still is then compared against a traditional flat-bottomed solar still, and modifications in the design are proposed to improve the production from the still and the usability of the still.

TABLE OF CONTENTS

ACKNOWLEDGEMENTS	i
ABSTRACT	ii
LIST OF TABLES	vi
LIST OF FIGURES	viii
ABBREVIATIONS	ix
NOTATIONS	x
1 Introduction	1
1.1 Introduction	1
1.2 Motivation	1
1.3 Schematic of a single-effect solar still	3
1.4 Objectives	3
1.5 Scope	3
1.6 Organisation of the report	4
2 Theoretical modeling and design analysis of a typical still	5
2.1 Introduction	5
2.2 Theoretical model of the still	5
2.3 Design parameters impacting the performance of the still	8
2.4 Distilled water vs potable water	9
3 Design of prototype 1	11
3.1 Introduction	11
3.2 Dimensions of the still	11
3.2.1 Flat-bottom solar stills	13
3.2.2 Inclined-basin solar stills	13

3.2.3	Comparison between flat and inclined bottom solar stills	13
3.2.4	Finalised basin dimension and shape	13
3.3	Selection of basin material	14
3.4	Supplementary material for augmenting heat absorption	15
3.5	Optimal angle of inclination	15
3.6	Design of thermal insulation for the still	16
3.6.1	Polyurethane (PU) Foam	16
3.6.2	Polystyrene - Expanded (EPS) or Extruded (XPS)	16
3.6.3	Fibreglass rolls and sheets	17
3.6.4	Wood fibre/shavings	17
3.6.5	Selected insulation material	18
3.7	Choice of top cover material	18
3.7.1	Transparent glass	18
3.7.2	Transparent polycarbonate (PC)	20
3.7.3	Polymethyl methacrylate (PMMA)	20
3.7.4	Selected material for the top cover	21
3.8	Optimal water depth for increased performance	21
3.9	Data acquisition for measuring performance	21
3.9.1	BMP180 pressure and temperature sensor	22
3.9.2	TMP36 temperature sensor	22
3.9.3	DTH22 relative humidity and temperature sensor	22
3.9.4	LM35 precision temperature sensor	22
3.9.5	Choice and placement of sensors	23
3.10	Summary	24
4	Modifications made in prototype 2	26
4.1	Introduction	26
4.2	Size of the water basin	26
4.3	Structural rigidity of the water basin	28
4.4	Design of top cover for easy assembly and usage	28
4.5	Temperature sensor selection and placement	29
4.6	Summary	31

5 Experiments conducted	32
5.1 Introduction	32
5.2 Basin bed temperature: sand against charcoal	32
5.3 Water evaporation with charcoal on the basin	34
5.4 Distilled water collection with regular water supply	36
5.5 Summary	36
6 Conclusions and possible extensions	40
6.1 Conclusion	40
6.2 Improved design	41
6.2.1 Adjustable basin inclination	42
6.2.2 Reflective cover for increasing solar energy input	43
6.2.3 Movable frame and basin	46
6.3 Future work	47
A The CAD drawings of the first prototype	48
A.1 Basin sheet metal bending drawing	48
B The CAD drawings of the second prototype	49
B.1 Basin sheet metal bending drawing	49

LIST OF TABLES

3.1	A parameter scoring analysis to evaluate the various materials. All scores are out of 10.	14
3.2	Common insulating materials, their R values, advantages and disadvantages (as reproduced from [1])	19
6.1	A comparison of the water output from the inclined basin prototyped in this work and a conventional flat-bottomed still discussed in [2]. . .	40

LIST OF FIGURES

1.1	A map showing the drought impacted regions in 2016 (as reproduced from: [3])	2
1.2	A simple schematic of a single basin solar still (as reproduced from [4])	3
2.1	A thermal of a single basin solar still (as reproduced from: [5])	6
2.2	Schematic showing the steady state heat flows for a single-effect solar still (as reproduced from: [6])	7
2.3	Ideal production rate as a function of radiation rate and ambient temperature (as reproduced from: [6])	8
2.4	Typical minerals found in drinking water (as reproduced from: [7])	9
3.1	A CAD model of the still, which was used for manufacturing the first prototype	11
3.2	A render of the CAD model of the first prototype showing the some of the variable dimensions.	12
3.3	The placement of the LM35 temperature sensors on the top view of the first prototype. The dots indicate the sensor position.	23
3.4	The procured LM35 temperature sensors in LP packaging. The exposed leads are a source of noise and susceptible to getting shorted by impurities.	24
3.5	The raw and filtered temperature data from the LM35 sensor.	25
4.1	A render of the two basins side by side.	27
4.2	A render of the second basin, indicating some of the critical attachments.	27
4.3	A render of the second basin showing the overlap provided for increased stiffness.	28
4.4	An image of the second basin showing the welded overlap provided for increased stiffness.	29
4.5	A render of the second prototype's basin with the top cover attached to a wooden frame.	30
4.6	A comparison of the raw data collected from the DS18B20 and LM35 temperature sensors.	30

5.1	The plots show the basin bed temperature against time, when charcoal and sand are used to improve the heat absorption.	33
5.2	A comparison of the basin bed temperature with and without water. Data collected on April 27th using DS18B20 sensors.	34
5.3	The amount of water collected from the still with charcoal on the still bed.	35
5.4	The container used to supply water to the still with the flow control pipes attached.	37
5.5	A comparison of the water surface temperature and top glass temperature. Data collected using DS18B20 sensors.	38
5.6	The amount of water collected from the still with charcoal on the still bed and a steady water supply provided to the basin.	39
6.1	A render of the improved model of the still with modifications made to enhance the performance.	41
6.2	A render showing the supporting frame for the basin.	42
6.3	A render showing the proposed angle adjustment mechanism.	43
6.4	A render showing the still model with the reflector attached.	44
6.5	A render showing the handle fixed to the reflective cover.	44
6.6	A reflective aluminium sheet attached to the still to increase the input solar energy to the still.	45
6.7	A render showing the wheels attached to the frame and the handles on the basin allowing for easy movement.	46
A.1	The 2D CAD drawing of the basin for the first prototype.	48
B.1	The 2D CAD drawing of the basin for the second prototype.	49

ABBREVIATIONS

DFMA	Design for manufacturing and assembly
WHO	World health organisation
CAD	Computer aided design
PU	Polyurethane
EPS	Expanded polystyrene
XPS	Extruded polystyrene
FRP	Fibre-reinforced plastic
PC	Polycarbonate
PMMA	Polymethyl methacrylate
OTS	Off the shelf
BOM	Bill of materials

NOTATIONS

C	Heat stored in the basin
C_g	Heat stored in the top glass cover
G_h	Solar radiation rate on horizontal surface, kW/m ²
G_T	Total solar radiation on horizontal surface, kJ/m ²
G_s	Solar (short wave) irradiation, Btu/hr ft ²
G_L	Atmospheric (long wave) irradiation, Btu/hr ft ²
M	Total mass of evaporated water, kgm ²
\dot{m}	Evaporation rate, kg/m ² s ²
q_k	Heat loss from still by conduction through base, Btu/hr
q_e	Heat transfer by evaporation
q_c	Heat transfer by convection
q_{cz}	Heat loss by convection to environment
q_r	Heat transfer by radiation
q_{rz}	Heat loss by radiation to environment
T	Temperature, °R
T_a	Temperature of ambient air, °R
T_g	Temperature of glass, °R
α	Absorptance of still base for solar energy
α_{gL}	Absorptance of glass cover for long wave radiation
α_{gs}	Absorptance of glass cover for solar radiation
α_w	Effective absorptance of the still
η_i	Internal still efficiency
η_o	Overall still efficiency
τ	Transmittance of transparent cover plus water film for energy
θ_s	Time from sunrise to sunset, hrs

CHAPTER 1

Introduction

1.1 Introduction

Potable water is highly scarce in many areas of rural India, and combined with a lack of stable electricity, presents an almost insurmountable challenge for people to source drinking water. The traditional method of digging wells is not viable any more in the face of dropping water tables, and a suitable, green alternative is needed to supply the bare minimum of 5 l per day water required per person for survival [8].

One simple and time-tested solution is harnessing the power of the Sun to evaporate and then re-condense water to purify it. It is proposed that solar stills explicitly designed for this purpose will be ideally suited for this purpose. The proposition of using a solar still is not new, and many researchers have been investigating the various ways in which the still can be designed to maximise the output. The different kinds of stills have been explored in [9, 10, 11].

The scope of this work has been limited to passive, single effect solar stills, based on the work of [2], wherein the various design parameters and their effect on the efficiency of the still have been explored. The underlying theory of the thermodynamic process is based on the work of [5], and the main aim of this project is to establish the optimal design parameters for single effect solar stills that produce an output of 5 L/m^2 per day. The design is to be verified by building a prototype and then perform a design for manufacturing and assembly (DFMA) analysis on it to achieve a pre-production prototype.

1.2 Motivation

India has a long coastline, roughly measuring 7516.6 km [12], and hence has an abundant supply of brackish water. However, many of the same areas face significant potable

water shortages, as shown in Fig. 1.1. This shortage is due to an inability to convert the contaminated brackish water to safe drinkable water. The reasons for this are manifold, some of the major ones are the absence of electricity or its reliable supply, prohibitively sparse availability and high cost of water purification, the scale of implementation, lack of a municipal supply and lack of awareness that contaminated water can be purified easily.



Figure 1.1: A map showing the drought impacted regions in 2016 (as reproduced from: [3])

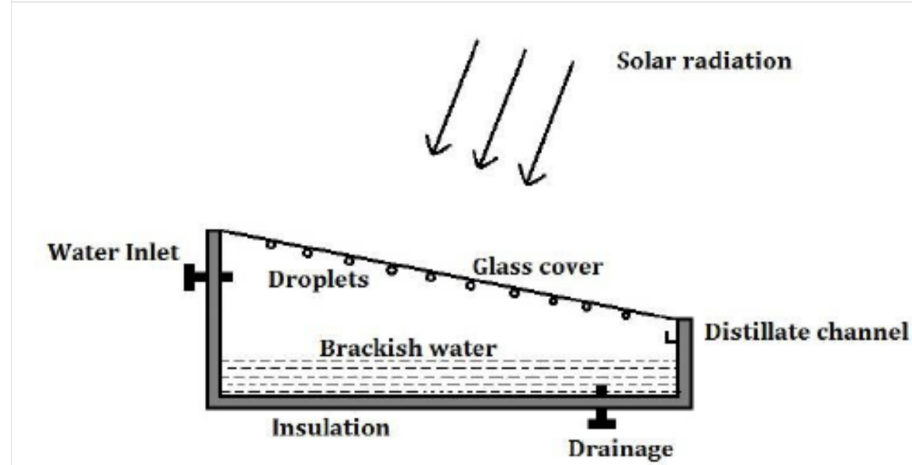


Figure 1.2: A simple schematic of a single basin solar still (as reproduced from [4])

1.3 Schematic of a single-effect solar still

A typical single-effect solar still is shown in Fig. 1.2, where the critical components are the top cover, basin, insulation around the basin, distillate collection channel, water inlet and the supply of contaminated water.

Each of the above is a variable design parameter that impacts the amount of distillate generated from the still. The various design parameters and other design considerations are discussed in the subsequent chapters in greater detail.

1.4 Objectives

The primary objective of this work is to design a product that can produce potable water above 5 l per day, which is shown to be enough for one person for one day [8], without requiring electricity or any other active energy source such as manual labour.

1.5 Scope

The scope of this work is limited to single-effect solar stills, due to the extensive research done in this domain, their proven ruggedness and performance and their not requiring any external power source.

The objective of this project work is, therefore, to determine the design parameters

that have the most significant impact on the performance of a solar still, and to develop an improved design of single effect solar stills that delivers at least an output of 5 L/m^2 per day.

1.6 Organisation of the report

This report is organised into six chapters. Chapter 2 details the theoretical model of a single-effect solar still, the design parameters that affect the performance of the still and the viability of distilled water as a source of potable water. Chapter 3 discusses the building of the first prototype, outlining the design decisions that were taken in the making of the prototype and the reasoning behind them. It also discusses some of the issues faced in the building of this prototype and the knowledge that can be carried forward to the second prototype. Chapter 4 discusses the changes made in this design iteration in greater detail and the challenges and feedback from the same. Chapter 5 details the various experiments that were conducted using these prototypes and discusses the results from the same. Chapter 6 consists of the results from the tests done and also outlines an improved design of the single-effect solar still that is easier to manufacture, assemble and maintain.

CHAPTER 2

Theoretical modeling and design analysis of a typical still

2.1 Introduction

Understanding the theoretical model of the still is as vital as developing a prototype, as it provides an insight of the functioning of the still and also aids in identifying the design parameters that have a significant impact on the performance of the still. It also gives a theoretical estimate of the efficiency of the still, providing a goal towards which the design can then aspire.

There are three primary processes taking place in single-effect solar stills, namely, the absorption of solar energy by the water in the basin, the evaporation of water from the basin, and the condensation of water on the roof of the still.

There are various secondary processes that directly or indirectly impact the above three, which are the reflection of solar energy by the top cover, the absorption and reflection of energy at the bottom of the basin and the absorption and loss of energy by the sides of the still.

A thermodynamic analysis of the above processes gives an understanding of the functioning of a still and helps in creating a mathematical model of the still that can be used to calculate the theoretical efficiency of the still.

2.2 Theoretical model of the still

The main body of work in establishing a mathematical model of the solar still was laid down by [5, 6]. The still, whose schematic is given in figure Fig. 1.2 is modelled as a thermal circuit shown in Fig. 2.1. The solar radiation incident on the top cover consists of short wave solar radiation, G_s , and longwave radiations G_L . The amount of

energy that passes through the cover is τG_s , where τ is a scalar and $\tau \in [0, 1]$. This is because most of the longwave rays are absorbed in the glass cover. Of this, the amount of solar energy that strikes the bottom of the still basin is $\alpha\tau G_s$, where α is a scalar and $\alpha \in [0, 1]$. This represents the amount of solar radiation absorbed per unit area of the still. The value of $\alpha\tau$ is approximated to 0.8 by [5], this value is also used in this work.

As seen in the thermal circuit in Fig. 2.1, of the energy impacting the bottom, q_k will be lost to conduction, some will be used up in heating the water and the remainder will be released from the water surface by convection, evaporation and radiation. This energy is then taken in by the lower surface of the top cover and is then lost to the environment by convection and radiation.

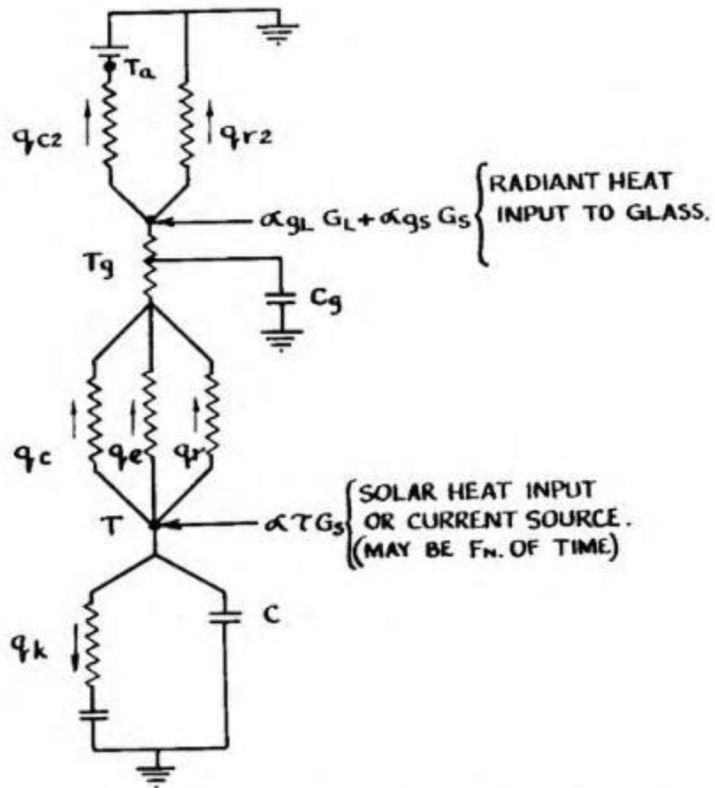


Figure 2.1: A thermal of a single basin solar still (as reproduced from: [5])

Based on this model, [6] has estimated the theoretical maximum efficiency of single-effect horizontal solar stills and has tested it against a prototype for verification and validation. The overall efficiency, η_o , and the internal efficiency of the still η_i , are mathematically defined as:

$$\eta_o = \frac{q_e}{G_h}; \quad (2.1)$$

$$\eta_i = \frac{q_e}{\alpha_w G_h}; \quad (2.2)$$

$$\implies \eta_o = \alpha_w \eta_i, \quad (2.3)$$

where α_w is the effective absorbtance of the still. α_w encapsulates the external solar radiation that is successfully absorbed and utilised in the heat transfer modes from the water in the basin.

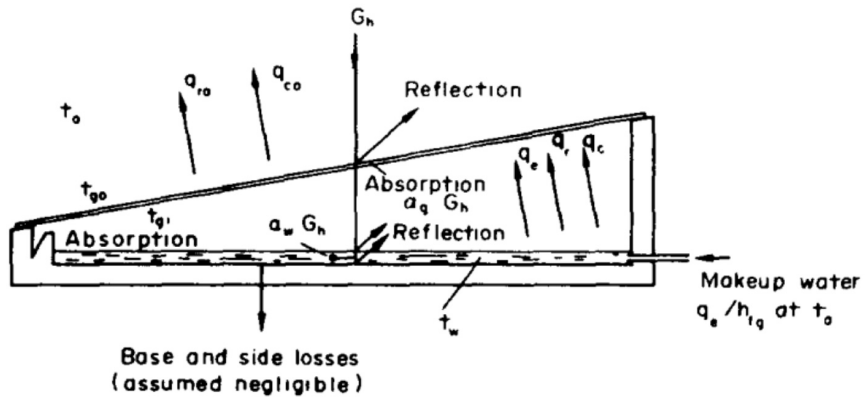


Figure 2.2: Schematic showing the steady state heat flows for a single-effect solar still (as reproduced from: [6])

Though, as [5, 6] were unable to find a theoretical solution for the governing set of equations, an iterative technique was used to calculate the *idealised* production rate for a given radiation rate and ambient temperature. The results are shown in the Fig. 2.3. The sharp boundaries for ambient temperatures of 20°C to 50°C represent a limiting water temperature of 90°C in each case. Thus, the ideal overall efficiency can be given as:

$$\eta_o = 0.727 - 2.88 \times 10^2 \frac{\theta_s}{G_T}, \quad (2.4)$$

where θ_s is the average duration for which the still is operational and G_T is the total solar radiation on a horizontal surface on an average.

The values of θ_s and G_T , when assumed to be 12h and 30×10^3 kJ/m² respectively,

results in an overall efficiency η_o of 61.2%. However, it is possible to measure short-term efficiencies that are greater than this figure with real systems that have thermal lag.

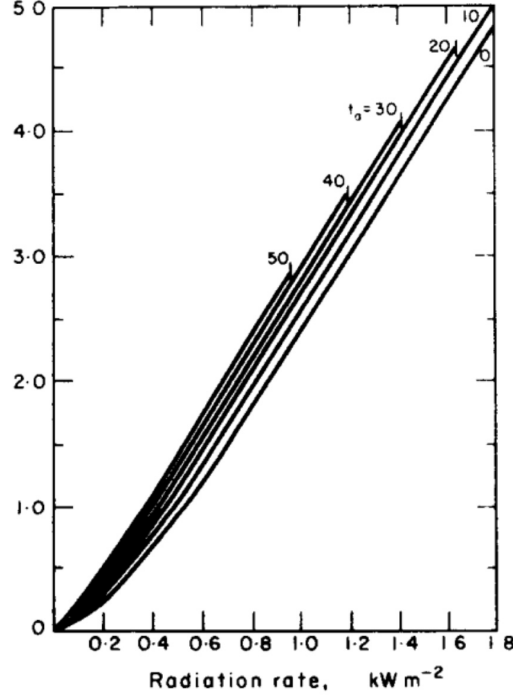


Figure 2.3: Ideal production rate as a function of radiation rate and ambient temperature (as reproduced from: [6])

When the value of the overall efficiency, η_o , was verified experimentally in [6], it was found that the empirical value of the overall efficiency was 51.3%, whereas the ideal theoretical efficiency was 57.3%. The possible reasons for this discrepancy are losses from the bottom and sides of the basin, thermal lag in the system and other non-ideal conditions that are unavoidable in real-world systems.

2.3 Design parameters impacting the performance of the still

The various design parameters that impact the performance of a solar still have been extensively tested by multiple authors [10, 11, 2, 13, 14, 15, 16, 17, 18]. The main design parameters are the solar radiation, wind velocity, ambient air temperature, brine depth, glass angle, size of the basin, material of the basin, walls of the container and the

addition of an external condenser.

2.4 Distilled water vs potable water

Bioavailability	Occurrence	
	Moderate Amounts in Some Supplies	Low Amounts in Most Supplies
High	Se* Na Cl F	P K* Mo I* B*
Moderate/Variable	Ca* Mg* Cu* Zn*	Mn
Low	Fe*	Cr

*sub-optimal consumption and/or prevalent deficiency in at least some countries

Figure 2.4: Typical minerals found in drinking water (as reproduced from: [7])

Production of potable water by desalination is an age-old method, and there are various processes to achieve this. Most of these are discussed in detail in [19]. There are various minerals that are typically found in drinking water around the world, these are shown in Fig. 2.4, as found in [7].

Distilled water is not deemed potable around the world, as there are various concerns regarding the safety and adverse health effects of the same. This aversion is based on various studies carried out by the World Health Organisation (WHO) when specifying the drinking water standards in [8]. The various dangers of consuming demineralised water are discussed in [20].

However, the notion that it is unsafe to consume desalinated water is being challenged again by further studies on the topic. New research conducted by the WHO [7, 21] shows that the specific minerals that impact the health of consumers are Magnesium, Calcium and Fluorine. There are few regions in the world where water is the primary source of these minerals [7]. Hence, in areas like India, where there is a high mineral salt intake, the low percentage of these minerals in the drinking water supply is not of significant concern.

What is a major concern is the aggressive nature of water low on minerals [22]. Such a water source is difficult to store and transport, as it attacks the containers and transmission piping, gaining unhealthy minerals that can cause harm. Hence, various remineralisation methods are recommended by the WHO [22], to make the water safe for storage and transmission.

CHAPTER 3

Design of prototype 1

3.1 Introduction

The theoretical efficiency of the still was calculated to be 57.3%, whereas the empirical efficiency was estimated to be 51.3% in section 2.2. However, these need to be realised to achieve the goal of producing 5 l of water per day.

Based on the model specified in Section 2.2 and the schematic outlined in Section 1.3, a Computer Aided Design (CAD) model of a single-effect solar still was made using Autodesk Fusion 360. A render of the model can be found in Fig. 3.1. The specifics of the CAD and hence the prototype are discussed in the subsequent sections.

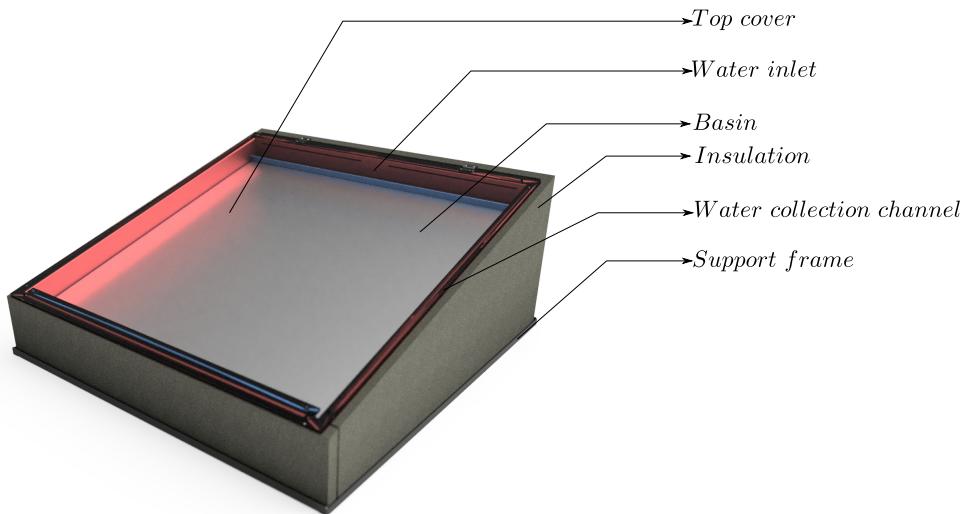


Figure 3.1: A CAD model of the still, which was used for manufacturing the first prototype

3.2 Dimensions of the still

The variable dimensions of the water basin are the length, breadth and height of the basin, the shape of the cross-section of the basin, the water ingress and egress points,

the water collection pathways and the thickness of the basin. Some of these have been illustrated in Fig. 3.2, and the complete engineering drawings of the model have been included in Appendix A.1.

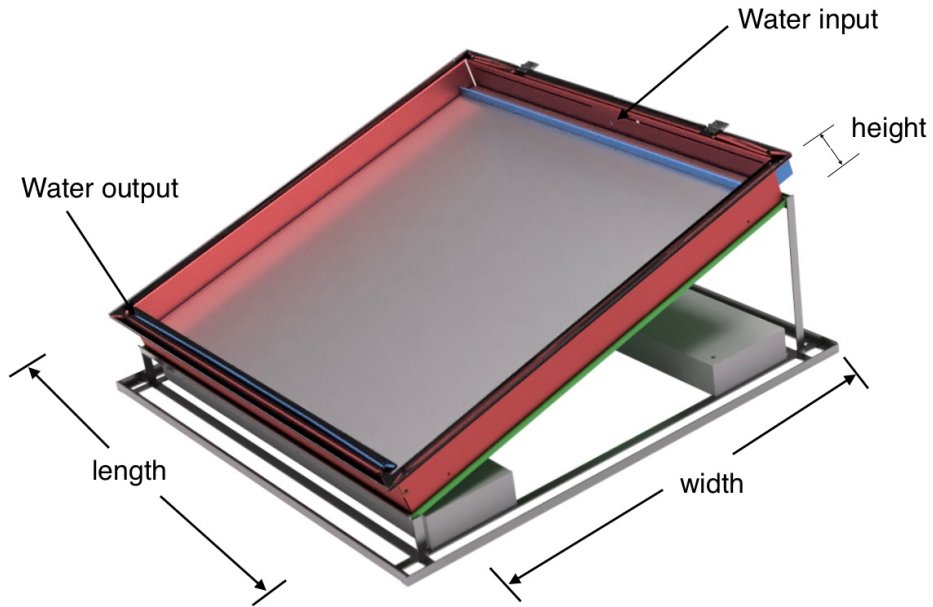


Figure 3.2: A render of the CAD model of the first prototype showing some of the variable dimensions.

It was determined from Section 2.2 that, for an order of magnitude of a few hundred to a few thousand mm, the lateral dimensions of the still do not have a significant impact on the performance of the still.

The metric based on which the still is evaluated is the amount of water produced per unit area per day, whose units are L/m^2 per day. Hence, to ease all further calculations and reporting of results, the length and breadth of the basin were selected to be 1 m each.

The height of the still was set to 100 mm to accommodate the water collection channels, inlet and outlet ports and the supplementary material added to enhance heat absorption.

3.2.1 Flat-bottom solar stills

Most stills are conventionally flat-bottomed, the chief reason for this seems to be to maintain a constant, shallow depth of water to heat. The other attraction appears to be the simplicity in design and construction.

3.2.2 Inclined-basin solar stills

Stills inclined at an angle can have an increased surface area of water in the same floor area, and most can improve this advantage by adding various gradient arresters to the surface of the basin. This inclination helps to increase the surface area of water, thereby directly increasing the rate of evaporation.

The main drawback here seems to be the careful calibration required in adjusting the input flow rate of water, which would otherwise lead to the pooling of water one end of the still. This wastage should be mitigated in the design to avoid wastage of input water and also increase the efficiency of the still.

3.2.3 Comparison between flat and inclined bottom solar stills

Upfront, the inclined still presents many advantages over the conventional, flat-bottomed still. Some of these are an increased surface area for absorption and a compact design that reduces the footprint of the sealed container.

A few of the disadvantages the inclined still against the standard, flat bottomed still are an increase in design complexity and a reduced gap between the roof and the basin which can reduce the temperature difference between the two surfaces.

3.2.4 Finalised basin dimension and shape

The inclined bottom solar still model was selected for implementation, mainly due to the reasons specified in Section 3.2.3, but also to mitigate the lack of sufficient literature that discusses the merits and demerits of this basin design.

3.3 Selection of basin material

The requirements from the basin material are that it should be a good conductor of heat, so that the heat is distributed evenly to the water on the basin, it should be easy to manufacture, be readily available and should be inexpensive.

The materials that were considered for this purpose were mild steel, stainless steel, aluminium, various plastics and wood.

Table 3.1: A parameter scoring analysis to evaluate the various materials. All scores are out of 10.

Parameters	Material				
	Mild steel	Stainless steel	Aluminium	Various plastics	Wood
Heat conduction (higher is better)	8	6	10	3	2
Manufacturability (higher is better)	10	8	9	10	9
Availability (higher is more easily available)	8	6	7	9	9
Cost (higher is cheaper)	7	5	3	8	9
Weight (higher is lighter)	4	5	8	9	6
Durability (higher is more durable)	8	8	9	4	5
Total score	45	38	46	43	40

Based on the analysis shown in Table 3.1, Aluminium was chosen as the basin material for the initial prototype. The manufacturing method selected for the basin was sheet metal bending, as the structure would be rigid as well as light-weight while remaining relatively cost-effective in manufacturing.

3.4 Supplementary material for augmenting heat absorption

Various materials have been considered for increasing the heat absorbed by the basin surface and hence the water on the basin. The effectiveness of using sand, sponges and wicks has been reviewed in [10]. Sponge cubes, gravel and cotton cloth have been tested and reported in [11]. Sand and charcoal have been explored in [2]. Some popular and effective choices from these are blackened jute fibres, sand and charcoal.

Sand and charcoal have been shown to be the most effective, hence are considered for further examination in this design iteration. A comparison experiment has been conducted between these two materials to find the more effective material. The methodology and results of the same are discussed in Section 5.2.

3.5 Optimal angle of inclination

The angle of inclination of the top transparent cover of the still is an important design parameter in that it directly impacts the amount of sunlight and hence the energy that enters the still. A significant side effect of the inclination is that it naturally guides any water that condenses on the top to collect on one end of the still, thus preventing it from falling back onto the basin.

Although the literature agrees that having an inclined top is beneficial, there is little consensus on the exact amount of inclination that should be present. A few sources suggest that a 45° angle is best for year-round performance, whereas others say that matching the latitude of the location in which the still is placed will result in an optimal output. Others state that having an angle of 15° is essential for maximising the production of the still.

The conclusion is that some amount of flexibility needs to be present in the design so that the angle can be changed based on the developing literature as well as the preference and location of the user. This freedom translates to an increase in design complexity but, for now, it seems to be a necessary concession to be made.

3.6 Design of thermal insulation for the still

The basin needs to be insulated on all sides apart from the top to increase the efficiency of the still, which means that insulating material needs to be added in the sides and the bottom of the still. There are various materials for this purpose; the materials being considered here are polyurethane, polystyrene, fibreglass and wood fibres.

The key parameter for the measurement of the insulating capacity of a material is its R-value [1, 23]; which is the materials thermal resistance per unit area. Its unit is $\text{m}^2\text{K/W}$. It is inversely related to the thermal conductivity of the material.

The various advantages and disadvantages of the aforementioned materials is discussed below. A summary of the same discussion is provided in Table 3.2.

3.6.1 Polyurethane (PU) Foam

This foam is used extensively in the building industry as insulation in the walls. It is readily available in the form of sheets and boards and can also be expanded in-situ for a better fit. It has a high R-value and is readily available commercially. It also has a low vapour absorption tendency and is resistant to other chemicals.

The advantages of using PU foam as the insulation material are that it is easy to install, and it has a low density hence will not add to the weight of the still. PU is also inert to water vapour, thus will not absorb water vapour from the atmosphere over time like some other materials that will be subsequently examined in detail.

The chief disadvantage of using PU foam is that it is an expensive insulation material, and will be a major contributor to the overall bill of materials (BOM) of the product.

3.6.2 Polystyrene - Expanded (EPS) or Extruded (XPS)

This material has a higher strength than PU foam and can be installed in-situ. However, it was discarded as an insulator due to its flammable properties and its chemical reactivity with fibre-reinforced plastic (FRP) installations.

The benefits of using Polystyrene are that it is readily available, and it is available in a wide range of densities and thicknesses. This provides a freedom while designing the insulation of the still. Similar to the PU foam discussed above in Section 3.6.1, polystyrene is also resistant to water vapour.

The disadvantage in using either of EPS or XPS is that polystyrene is not a chemically inert material. Thus it has a tendency to breakdown when exposed to sunlight. If this material is chosen, there would be an increase in the design complexity, as the insulation would have to be covered completely to block sunlight. Another major drawback of this material is that it is flammable, hence poses a safety risk as well.

3.6.3 Fibreglass rolls and sheets

Fibreglass is made using recycled glass and binder material and made into rolls and mats. It is a prevalent material used predominantly in insulating homes and other buildings.

The advantages of using fibreglass are that it is flame retardant and chemically inert. This liberates the insulation design from having to account for foreign elements attacking and degrading the insulation. It is also cheap, and readily available in various forms such as rolls and sheets. This aids the manufacturability and assembly.

The demerits of using fibreglass are few but significant. The main drawback is that it absorbs water vapour very quickly from the atmosphere, and also loses its thermal resistance when wet. This severely degrades its performance as an insulating material. Designing around this caveat will increase the design complexity as well as the manufacturing complexity, which will push up the cost of the end product. It also has weak structural strength in most of its commercially available forms and tends to settle down over time under the influence of gravity. Hence, it would also have to be reinforced.

3.6.4 Wood fibre/shavings

Wood fibre is made either from new or recycled wood and is readily available, environmentally safe and easy to install. It is also available in a variety of forms such as boards, mats and loosely packed lumps.

The primary benefits of using this material are that it is cheap and readily available in a wide variety of boards and shavings. This makes it a popular material for indoor panels and false ceilings.

The predominant drawback of using wood fibre is the same as that of fibreglass outlined in Section 3.6.3; it absorbs water vapour quickly from the atmosphere and subsequently loses its insulating properties. It also has a higher density as compared to the other materials under consideration and would significantly contribute to the overall weight of the product if it were to be used.

3.6.5 Selected insulation material

The materials mentioned above and their properties are summarised in Table 3.2. Based on this, the insulation material chosen was PU foam for its high R-value that enables a thinner insulation setup and helps keep the weight of the product down.

3.7 Choice of top cover material

The top cover is one of the most critical elements of the still; it is where one of the important thermodynamic processes mentioned in Section 2.1 takes place, namely, the condensation of evaporated water. It is also the primary inlet of solar energy into the still, and hence regulates the efficiency of the still directly. Therefore the choice of material of the top cover is a significant design decision.

3.7.1 Transparent glass

Glass is an established material that has very good transmissivity and thermal properties, being able to function at high temperatures without deforming. They also have very high longevity as compared to other materials.

The advantages of using glass as the top cover material are that it has a high transmissivity across the light spectrum, and is cheap and readily available. Glass also has a high thermal resistance to colourise under continued exposure to light. It also does not distort or deform under thermal load as much as the other materials under consideration.

Table 3.2: Common insulating materials, their R values, advantages and disadvantages
 (as reproduced from [1])

Insulating material	"R" value per inch	Advantages	Disadvantages
Polyurethane, board	6.25	Very good R-value, can be used with fibreglass resins	Not always easily available, relatively expensive
Polyurethane, spray on	7.0	Very good R-value, can be used with fibreglass resins, easy application with spray equipment	Not always easily available, expensive, requires special spray equipment
Polystyrene, sheets (smooth); trade name Styrofoam	5.0	Readily available, low cost, reasonable R-value	Cannot be used with fibreglass resins unless protected, easily damaged
Polystyrene, foamed in place and expanded moulded beads. Known as Isopor, Polypor, etc.	3.75 to 4.0	Reasonable R-values, lower cost than smooth surfaced sheets	Cannot be used with fibreglass resins unless protected, easily damaged
Fibreglass wool batts	3.3	Low cost, ease of installation	Readily absorbs water or other fluids, loses insulating value when wet
Wood shavings	2.2	Readily available, low cost	Absorbs moisture and loses R-values when wet, decays

The disadvantages of using glass for the top cover are twofold. The first is that the material is inherently very brittle, which makes it challenging to handle and manufacture. The second is that glass has a very high density, making it a significant contributor to the overall weight of the product.

3.7.2 Transparent polycarbonate (PC)

PC is another established material used most in the automotive industry for headlamp covers. It came up as an alternative to glass to mainly counter the highly fragile nature of glass.

The main advantages of using PC are its high strength, load-bearing capacity, and elasticity that make it a suitable replacement for glass where impact resistance is required. PC also has higher longevity as compared to other plastic-based transparent materials, thus making it more ideal for outdoor applications. Moreover, PC is lightweight and easy to machine, making it suitable for manufacturing, assembly, and improving the usability of the product.

The disadvantages of using PC are that it has a lower transmissivity as compared to glass, and it is also less hydrophilic when compared to glass. It also tends to turn yellow over time when exposed to sunlight for long periods, though the timeline for the colouration is around ten years. PC is also more expensive than glass, especially in small batches.

3.7.3 Polymethyl methacrylate (PMMA)

More commonly known as plexiglas, PMMA is a standard transparent plastic found mainly in buildings as an alternative to glass panes in windows and panels.

The benefits of using PMMA are that it is lighter than glass and also has higher load capacity and impact strength. The material is also cheap and more readily available as compared to PC. It is also lightweight and can be re-polished to restore its surface finish.

The primary disadvantage of PMMA is that it has a low operating temperature, making it unsuitable for this application. It also faces the same yellowing issues as PC,

as mentioned in Section 3.7.2, though PMMA degrades much faster than PC.

3.7.4 Selected material for the top cover

The factors that are taken into consideration in the selection of the top cover material are the transmissivity, impact strength, density, price, longevity and operating temperature of the material.

Based on these factors, the material that was chosen for the top sheet of the solar still is glass, as it offers the best trade-off between the various factors mentioned above.

3.8 Optimal water depth for increased performance

As has been shown in [2], the water depth at the bottom of the flat-bottomed still should be minimised for optimal performance of the solar still. However, this parameter does not directly translate to an inclined basin, as the inclination of the basin ensures that no water stagnates at any point on the base plate of the basin. Hence, the water depth is decided by the angle at which the corrugated aluminium sheet is folded, and the angle of inclination of the still.

3.9 Data acquisition for measuring performance

The performance of the still is directly evaluated based on how much water it produces. Hence, tracking this parameter provides a complete and accurate measure of the output of the still. However, to evaluate the efficiency of the still, a measure of the input energy into the still is also required. This need leads to some indirect parameters that can be measured which provide an insight into the efficiency of the still, namely, the temperature at various points on the still and the relative humidity inside the basin.

There are various off the shelf (OTS) sensors that can measure these parameters; they are discussed below.

3.9.1 BMP180 pressure and temperature sensor

This sensor from Bosch measures atmospheric pressure as well as temperature [24]; this will help in recording the pressure and temperature inside the chamber. It has a pressure measurement range of 300-1100 hPa (9000 m to -500 m above sea level), and a temperature range of -40°C to 85°C with an accuracy of $\pm 2^\circ\text{C}$ over this range. This sensor is moisture sensitive, and hence it cannot be used when placed on the bed. The placement needs to be carefully decided in the design phase.

3.9.2 TMP36 temperature sensor

This sensor is a dedicated temperature sensor, and is very small and compact [25], and is factory calibrated. It has a measurement range of -40°C to 100°C, and provides an accuracy of $\pm 2^\circ\text{C}$ over this range. Hence it can be used readily in places that require only a temperature reading.

3.9.3 DTH22 relative humidity and temperature sensor

This sensor measures relative humidity and temperature, and has a humidity range of 0-100% with a sampling rate of 0.5 Hz [26]. The operating temperature is up to 125°C. This sensor is not to be confused with the DTH11, which only has an operating temperature range of up to 50°C, as the temperature inside the chamber, which is at around 70-80°C at its highest, needs to be measured.

3.9.4 LM35 precision temperature sensor

This is a precision integrated-circuit pre-calibrated centigrade temperature measurement device developed and manufactured by Texas Instruments. It has a measurement range of -55°C to 150°C with a resolution of 0.5°C and a linear scale factor of 10 mV/°C [27].

3.9.5 Choice and placement of sensors

The parameters that were considered when selecting the sensor for data acquisition are temperature range, resolution of the sensor and the calibration (factory calibrated or not).

The LM35 temperature sensor by Texas Instruments was selected for measurement of temperature at various points on the still.

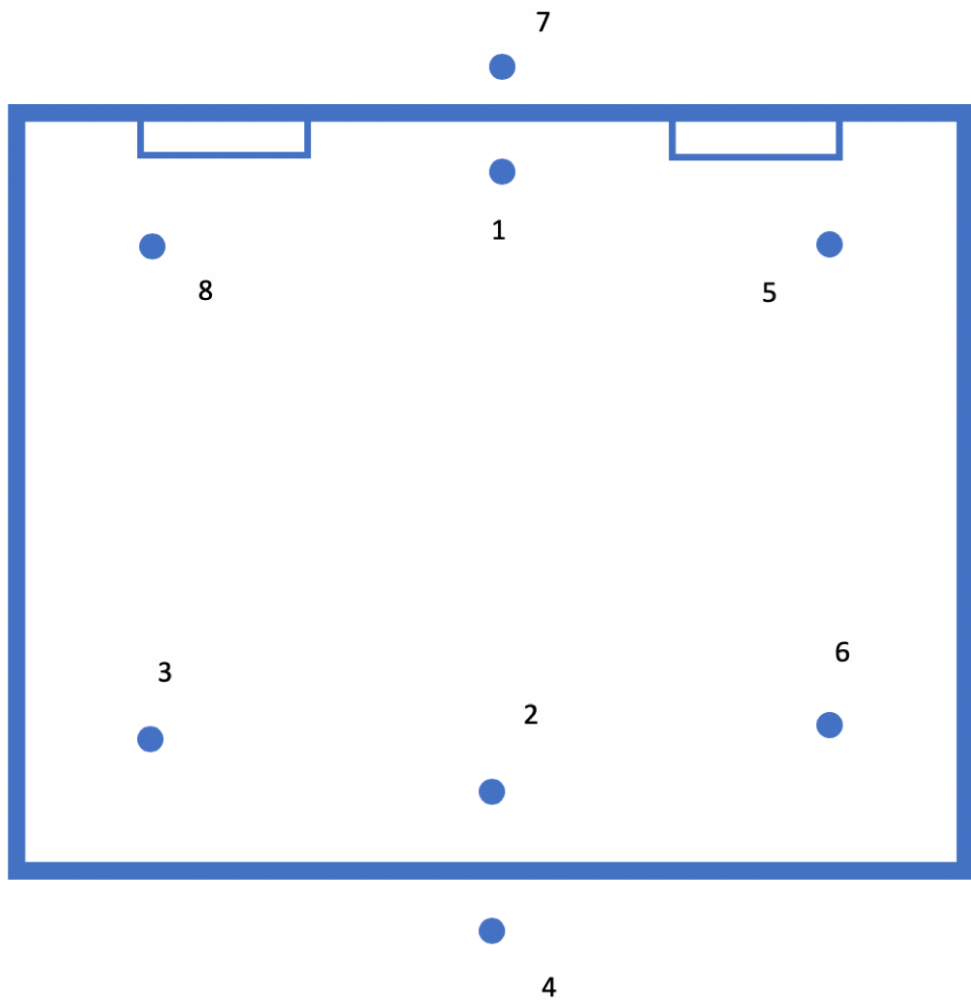


Figure 3.3: The placement of the LM35 temperature sensors on the top view of the first prototype. The dots indicate the sensor position.

The placement of the sensors is shown in Fig. 3.3. Sensors 1, 2, 4 and 7 are placed on the glass, with 1 and 2 on the inside of the top cover and 4 and 7 on the outside. The other sensors are attached to the underside of the basin of the still.

3.10 Summary

The building of this prototype highlighted some issues that were overlooked in the CAD design phase and while selecting the various materials and sensors. These were the size of the basin, the structural rigidity of the basin, the top cover assembly and the LM35 temperature sensors that were chosen for the temperature collection.

Owing to the large dimensions (1000 mm by 1000 mm) and the small thickness of the Aluminium sheet metal (2 mm), there is a large amount of flex in the basin. This flexing causes the basin to easily deviate from the horizontal, hence making the water flowing in the basin to escape from one of the sides without uniformly wetting the entire width of the basin.

The top cover of the first prototype is made entirely of plain glass, which makes it fragile and challenging to handle while removing to access the inside of the solar still. It also makes it difficult to make any modifications in the prototype as it is tough to machine glass without specialised tools that are expensive and uncommon.

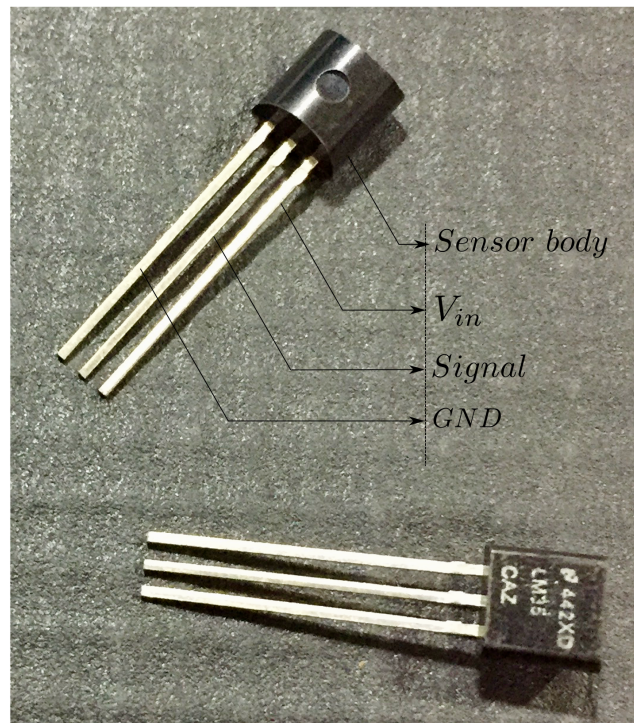


Figure 3.4: The procured LM35 temperature sensors in LP packaging. The exposed leads are a source of noise and susceptible to getting shorted by impurities.

The selected LM35 temperature sensors proved to be extremely noisy due to the exposed leads shown in Fig. 3.4. This resulted in erratic data from the sensors, requiring filtration of the sensor output data for further use.

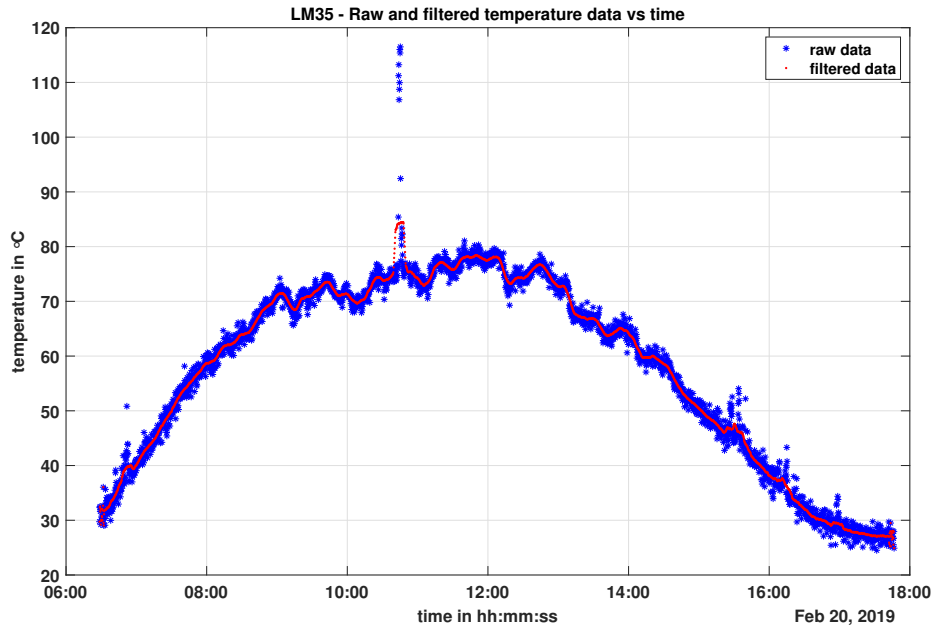


Figure 3.5: The raw and filtered temperature data from the LM35 sensor.

A comparison of the raw and filtered data is shown in Fig. 3.5 to illustrate the noise that is present in the sensor data. This is later compared, in Section 4.5, against the replacement temperature sensor data to show the difference between a sensor with protected leads and one without shields.

CHAPTER 4

Modifications made in prototype 2

4.1 Introduction

A second prototype was built to carry out comparative experiments between the various design factors mentioned in Section 2.3. The objective here is to implement/change a design element, for example, the addition of an external condenser, in one prototype and check the impact on the performance of the still against the other prototype that does not have that specific element.

This chapter outlines the changes that were made in the second prototype based on the feedback from the first prototype that are described in Section 3.10, namely, the size and structural rigidity of the basin, the design of the top cover and the sensors used to measure the temperature of the basin and top cover.

4.2 Size of the water basin

The size of the second basin was made smaller than the first basin, to address the portability and flex in the first prototype. As compared to the size of the first prototype, 1000 mm × 1000 mm × 100 mm (refer Section 3.2), the second basin was designed to be 800 mm × 800 mm × 100 mm, to improve the mobility of the still without compromising on the functionality and performance.

A comparison of the two basins is shown in Fig. 4.1, where the first prototype can be seen in red and the second in blue. A stand-alone render of the second prototype basin can be seen in Fig. 4.2, with some of the components labelled for the reference of the reader. A detailed 2D drawing of the same can be found in Appendix B.1.

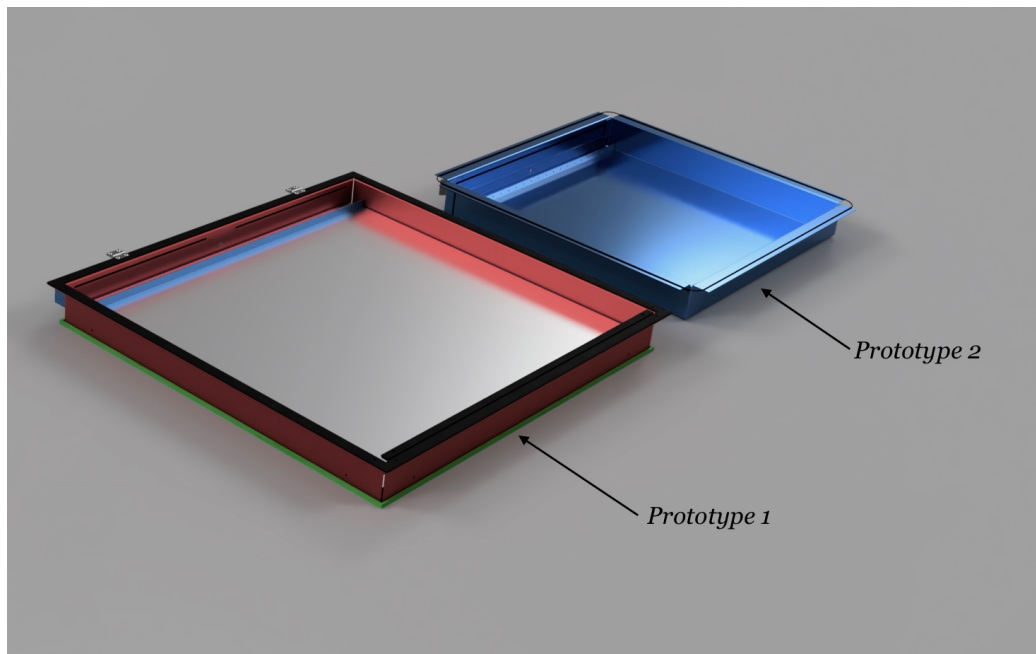


Figure 4.1: A render of the two basins side by side.

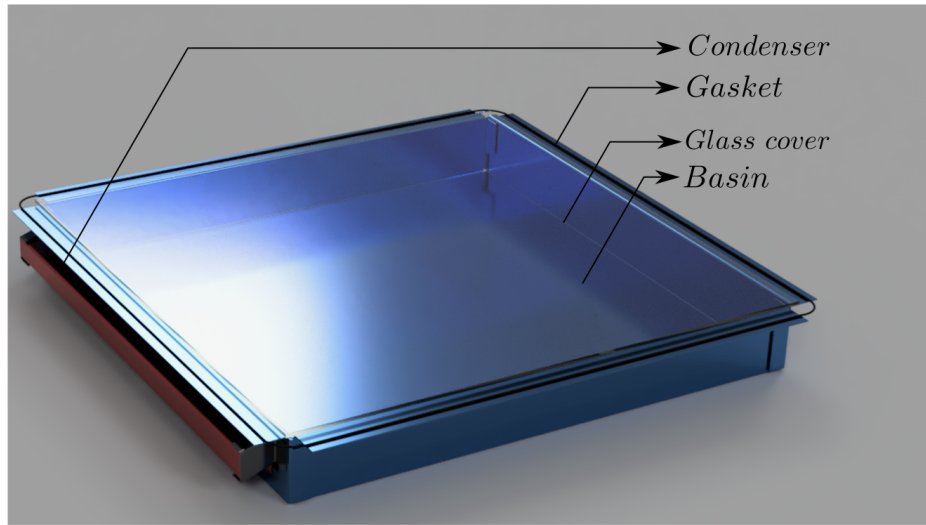


Figure 4.2: A render of the second basin, indicating some of the critical attachments.

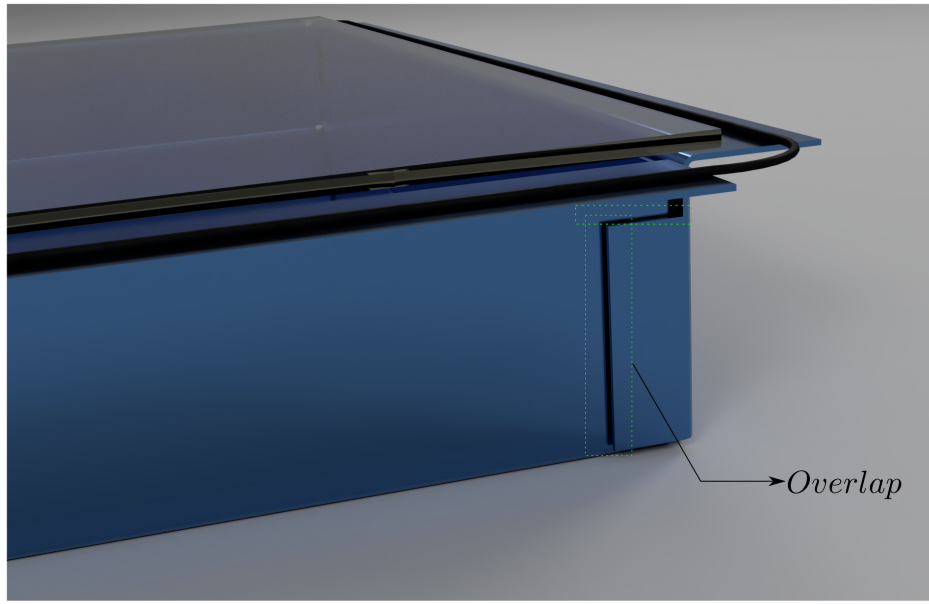


Figure 4.3: A render of the second basin showing the overlap provided for increased stiffness.

4.3 Structural rigidity of the water basin

The structural rigidity of the basin was improved by reducing the size of the basin, but it was decided to further bolster the basin by providing overlaps at the edges of the basin and then welding the same. The weld was achieved by Aluminium TIG welding [28, Chapter 6] along the overlapping edges. A render of the CAD model showing the overlap is shown in Fig. 4.3, and the welding can be seen in an image of the fabricated prototype in Fig. 4.4. It should be noted that the welding does not guarantee a fully water-sealed basin. Hence additional sealing needs to be provided either on the outside or the inside of the basin.

4.4 Design of top cover for easy assembly and usage

The top cover of the first prototype did not have any protection against damage along its edges and rested directly against the rubber gasket. The sides made it very difficult to make any adjustments to the glass cover after the glass had been cut. To mitigate these issues, modifications were made to the glass cover in the second prototype, wherein a

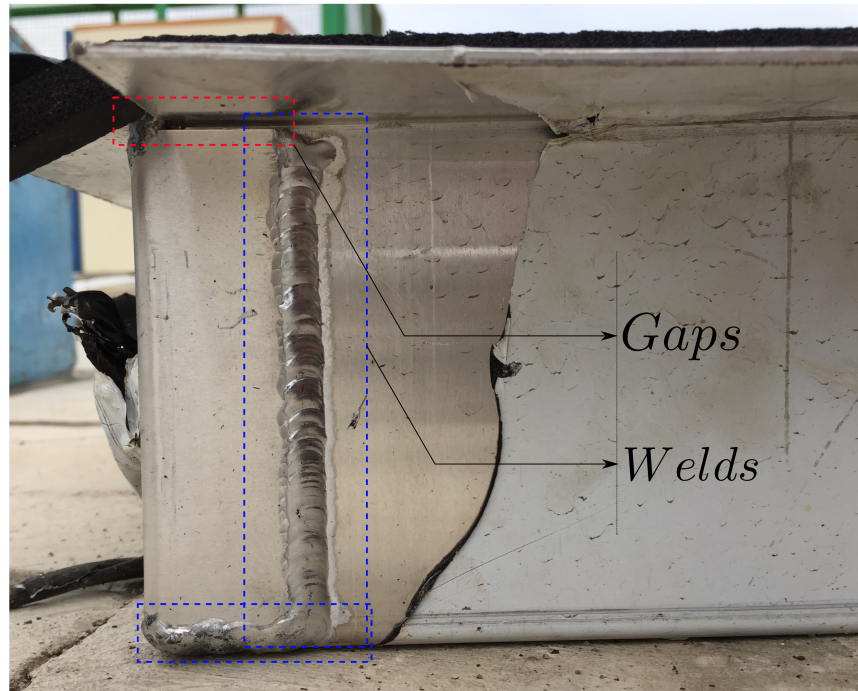


Figure 4.4: An image of the second basin showing the welded overlap provided for increased stiffness.

frame was attached to the cover.

A render of the basin with the top cover attached to the basin is shown in Fig. 4.5, it can be seen that the cover with the frame has better protection against impact, and it makes the top cover easier to handle and make post-manufacturing adjustments.

4.5 Temperature sensor selection and placement

The noise seen in the temperature data collected from the LM35 sensor makes it challenging to analyse the data and draw accurate inferences from it. To tackle this issue of excessive noise, the temperature sensor was changed to DS18B20. This sensor has a measurable temperature range of -55 °C to 125 °C and has an accuracy of ± 0.5 °C in the range of -10 °C to 85 °C [29].

A comparison test was conducted between the two sensors to illustrate the difference in the amount of noise carried in the two signals. The signal from the LM35 sensor has a large amount of variance and also has many outliers across the time range. On the other

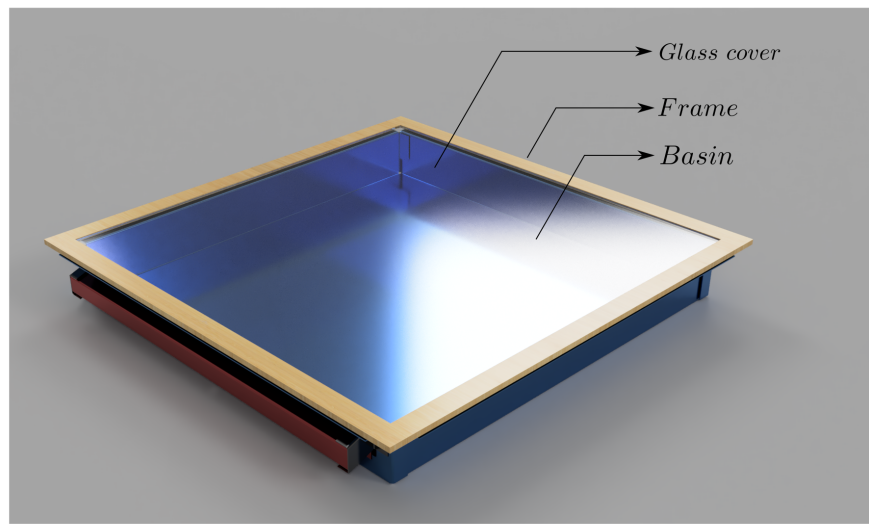


Figure 4.5: A render of the second prototype's basin with the top cover attached to a wooden frame.

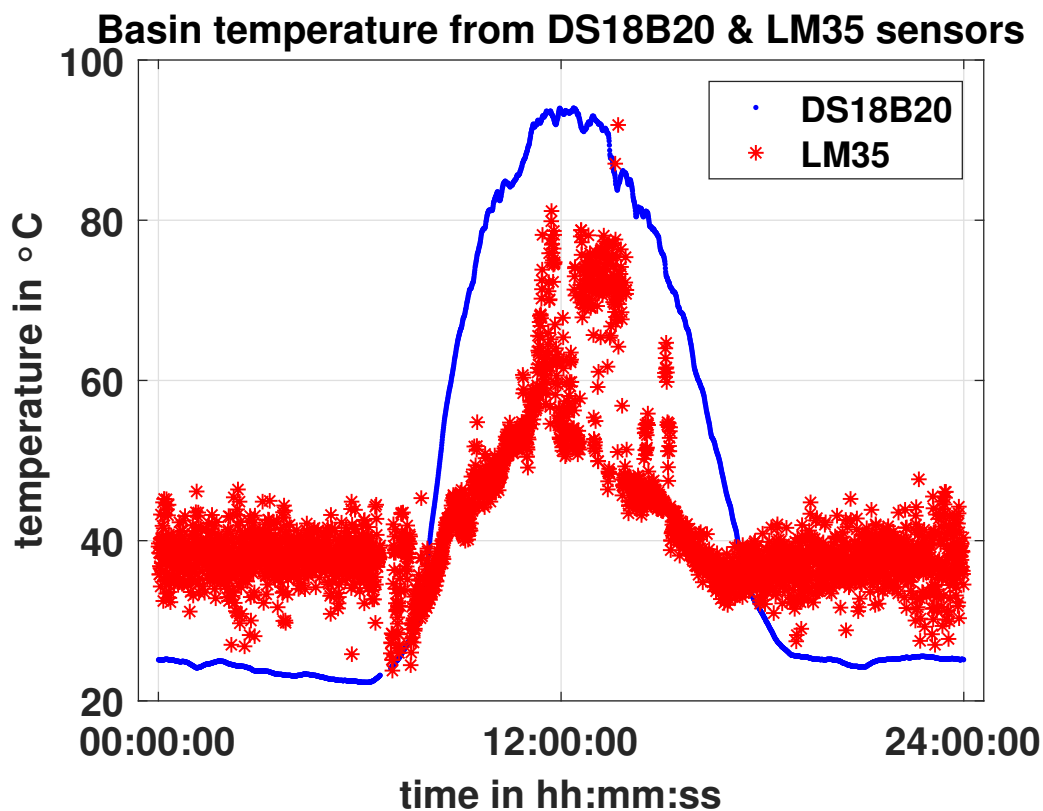


Figure 4.6: A comparison of the raw data collected from the DS18B20 and LM35 temperature sensors.

hand, the data from the DS18B20 sensor does not show any of these characteristics and has a smooth data curve across the entire time range.

4.6 Summary

The structural changes made in the second prototype cannot be transferred to the first prototype, but replacing the sensors on the first was a trivial venture and was done as soon as the superiority of the DS18B20 sensors was established. This enables uniform data collection from both prototypes, which can help gather more robust temperature data that is independent of the actual basin condition.

CHAPTER 5

Experiments conducted

5.1 Introduction

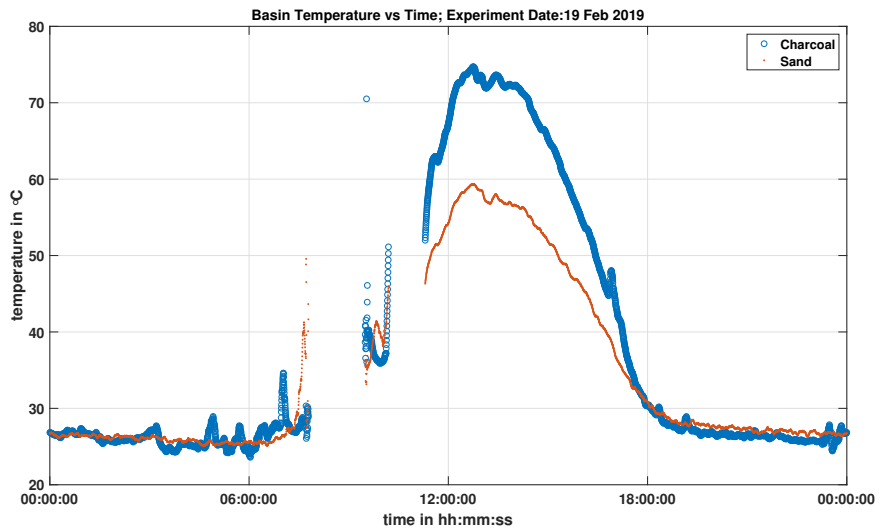
The impact of a few of the design parameters that affect the performance of the still, as mentioned in Section 2.3, are investigated in this chapter. In particular, the effects of the radiation absorption materials (sand and charcoal) discussed in Section 3.4 are investigated to decide on the better material. The performance of the still without any additional appendages such as a water supply reservoir, a water condensation apparatus and a reflector surface is investigated. It is compared against adding a continuous water supply to the basin that helps maintain a minimum water depth in the basin.

5.2 Basin bed temperature: sand against charcoal

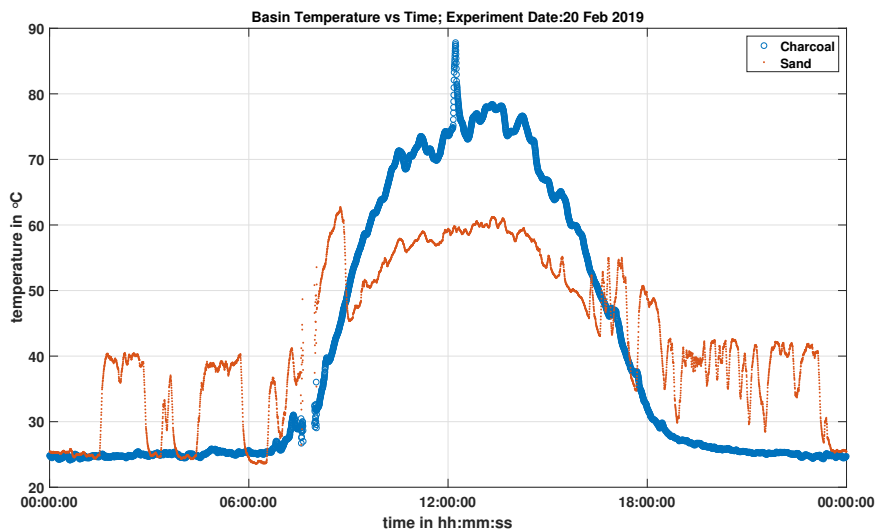
The basin was split into two halves vertically, and sand and charcoal were added to augment the heat absorption on these two surfaces. The aim was to see which material could take in more heat and thereby reach a higher temperature.

The experiment was conducted on the first prototype, and the data was collected using the LM35 sensor.

The results of the experiment can be seen in Fig. 5.1, where the data from tests conducted on February 19 and February 20, 2019, have been plotted against time. It can be seen that the temperature attained on the portion of the basin with charcoal on it is at least 10 °C higher than that on the surface with sand on it. This is significant as the temperature difference is directly proportional to the rate of evaporation from the basin of the still.



(a) Data collected on 19th February.



(b) Data collected on 20th February.

Figure 5.1: The plots show the basin bed temperature against time, when charcoal and sand are used to improve the heat absorption.

5.3 Water evaporation with charcoal on the basin

An experiment was conducted to see the impact of adding water to the still basin on the temperature of the basin. Charcoal was added to the basin bed to increase the heat absorption, as shown in Section 5.2. The temperature sensor used to measure the temperature was the DS18B20 sensor, due to the characteristics discussed in Section 4.5.

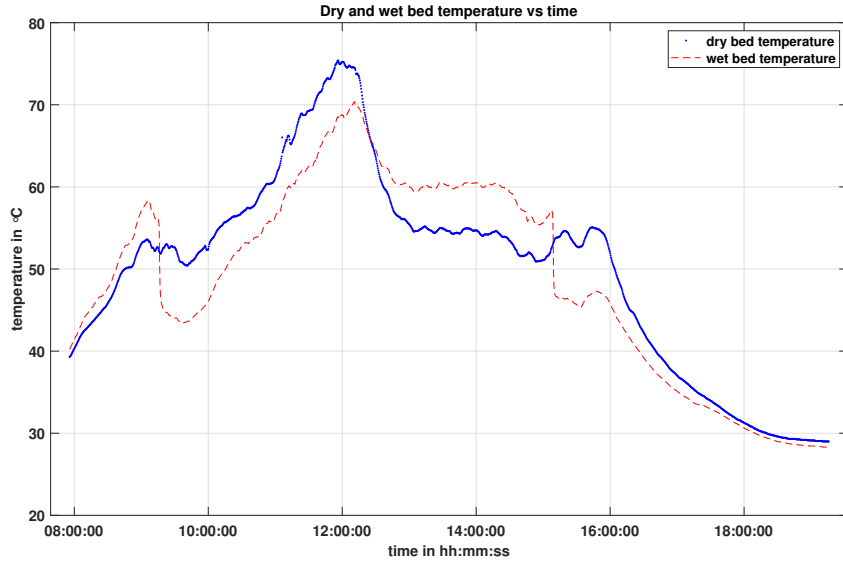
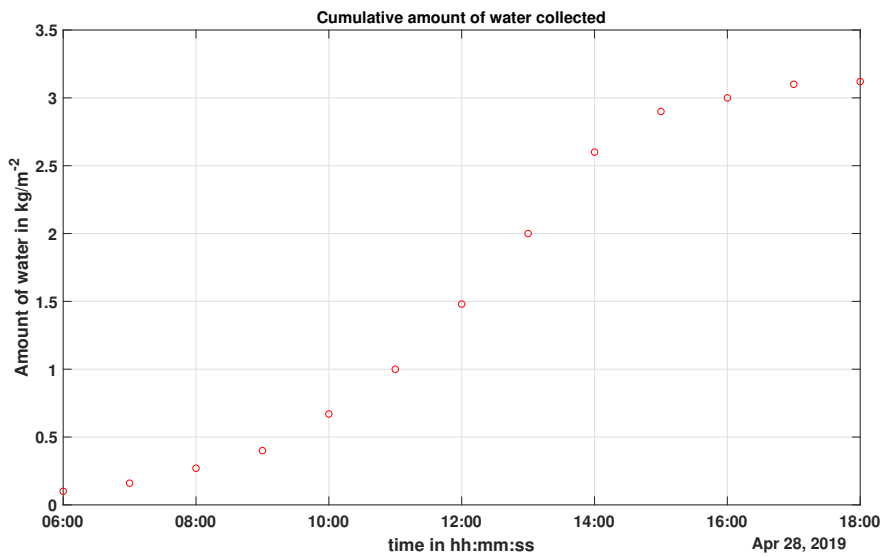


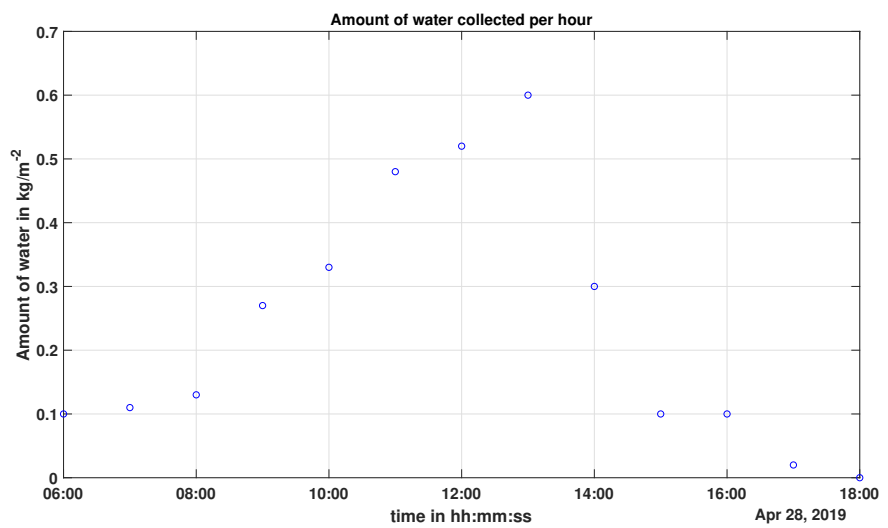
Figure 5.2: A comparison of the basin bed temperature with and without water. Data collected on April 27th using DS18B20 sensors.

The plots of the dry and wet bed temperatures against time are shown in Fig. 5.2. It can be seen that the wet bed temperature varies from the corresponding dry bed values by about 5 °C, the water being cooler when heating up and warmer when cooling. This is due to the high specific heat capacity of water (4.19 kJ/Kkg) [30] as compared to charcoal (1 kJ/Kkg) [31].

The amount of water collected during this experiment is slightly more than 3 L/m², and is plotted against time and shown in Fig. 5.3. The data was collected using a WeiHang portable electronic scale, which has a measurement range of 0 kg to 50 kg, and a resolution of 0.01kg [32].



(a) A cumulative measure of the amount of water generated from the still.



(b) A measure of the rate of water generated by the still per hour.

Figure 5.3: The amount of water collected from the still with charcoal on the still bed.

5.4 Distilled water collection with regular water supply

The amount of water condensed and hence extracted from the solar still is dependent on the difference between the temperature at which the water is evaporating and the temperature of the glass cover underside where it is getting condensed. The greater this gap, the greater the amount of water that is condensed and then collected. This is why the addition of an external condenser is effective in improving the performance of the still [2, 11].

The water supply attached to the still is shown in Fig. 5.4. A plastic container was used to store the water, and drip lines from medical saline tubes were used to regulate the water flow to the basin. The flow rate of water was adjusted to minimise the water run-off from the bottom of the still.

The temperature plots of the water on the bed of the basin and the glass surface against time can be found in Fig. 5.5. It can be seen that during the afternoon when the temperatures of both surfaces are at their maximum, there is a 5 °C difference between the glass and water temperatures. This difference increases to about 10° after this due to an increase in the wind velocity that cools the glass surface.

The water collection plots are shown in Fig. 5.6, about 3.8 L/m² per day was produced by the still. The water production rate was highest in the afternoon, between 12:00 pm and 2:00 pm, when the temperature difference between the water bed and the glass surface, seen in Fig. 5.5, was highest.

5.5 Summary

The above experiments show that the performance of the inclined-basin solar still is improved by the addition of the radiation absorption material and the continuous water supply. The water output from adding the charcoal to the basin (3 L/m² per day), seen in Fig. 5.3, and adding a continuous water supply (3.8 L/m² per day), seen in Fig. 5.6, significantly increased the output from the still. However, this quantity is still less than the desired target value of 5 L/m² per day, which, as mentioned in Section 1.1, is the bare minimum required for a person.



Figure 5.4: The container used to supply water to the still with the flow control pipes attached.

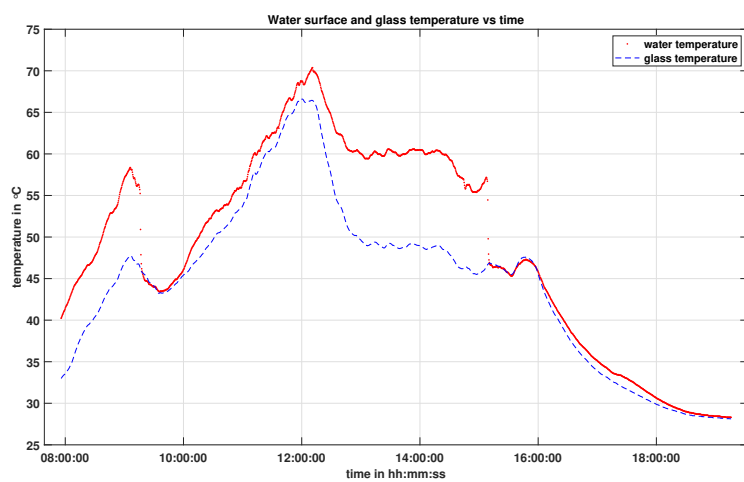
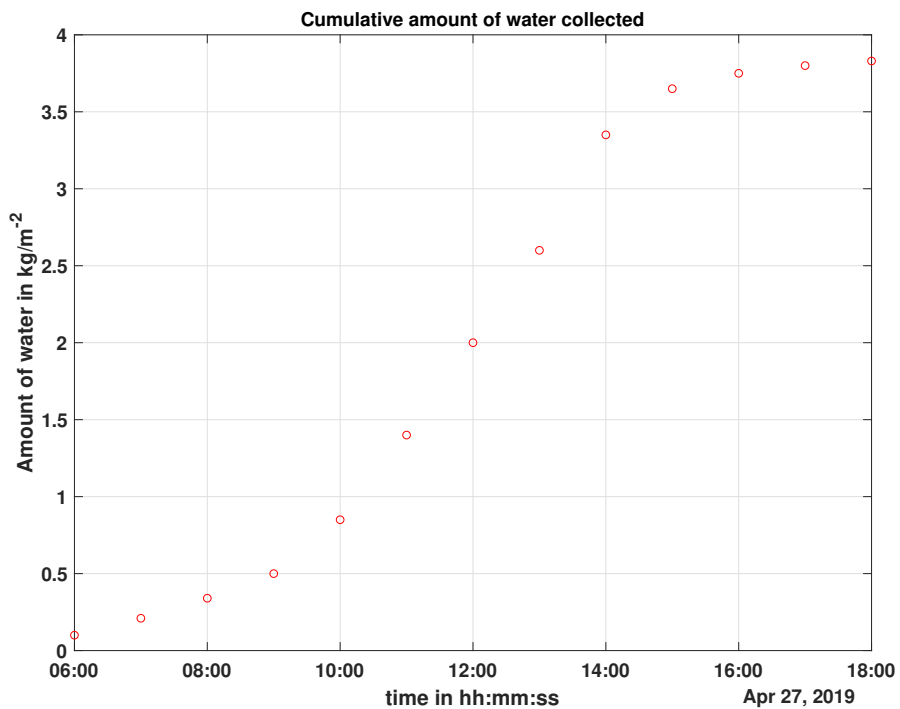
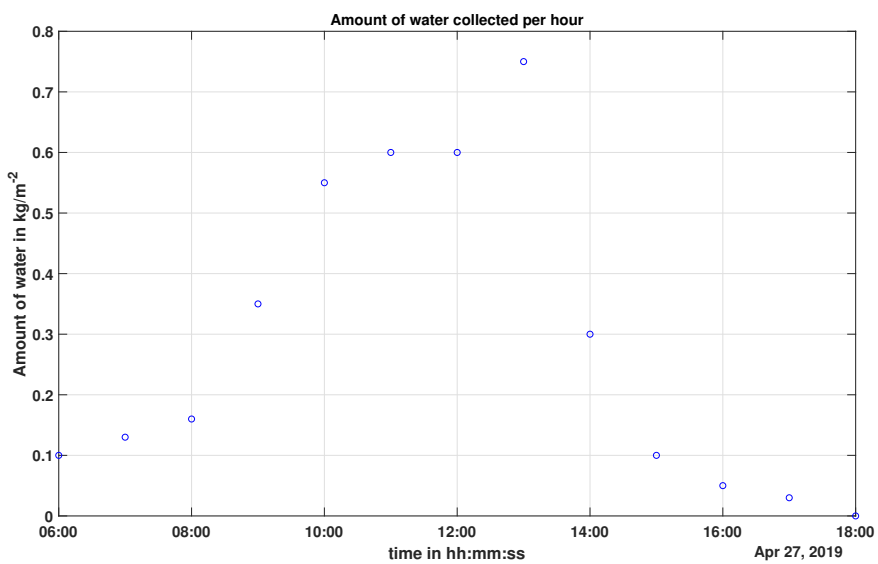


Figure 5.5: A comparison of the water surface temperature and top glass temperature.
Data collected using DS18B20 sensors.



(a) A cumulative measure of the amount of water generated from the still.



(b) A measure of the rate of water generated by the still per hour.

Figure 5.6: The amount of water collected from the still with charcoal on the still bed and a steady water supply provided to the basin.

CHAPTER 6

Conclusions and possible extensions

6.1 Conclusion

The experiments conducted in Chapter 5 show that the output from the still compares favourably with traditional flat-bottomed single effect solar stills. When compared with the solar still discussed in [2], the inclined basin still developed here outperforms its flat-bottomed counterpart when parity is maintained in the features and modifications made to the still.

Table 6.1: A comparison of the water output from the inclined basin prototyped in this work and a conventional flat-bottomed still discussed in [2].

Still operational condition	Inclined-basin solar still output (in L/m ² per day)	Flat-bottom solar still output (in L/m ² per day), as sourced from [2]
Basin with charcoal	3.1	2.2
Basin with charcoal and continuous water supply	3.8	4.2

A summary of the comparison of the two stills is shown in Table 6.1. The still with charcoal added to the basin, to augment the heat absorption, produces 2.2 L/m² [2] in case of the flat bottomed still with a water depth of 5 mm; whereas the inclined still produces 3.1 L/m² in the inclined-basin solar still.

When a reservoir is added to the still, a similar observation can be made. The flat-bottomed still produces 4.2 L/m² [2] when a water supply is added to it along with a mirror to increase the amount of incident sunlight. On the other hand, the inclined still

produces only 3.8 L/m^2 when a reservoir is attached to it. However, there is no mirror appended to increase the incident light.

These results show that, though the inclined-basin solar still is more difficult to manufacture, it has the potential to surpass the flat-bottomed still in terms of water output if suitable modifications are made to it. Some typical appendages that are added to improve the performance of a solar still are a reflector to increase the amount of incident light, and a condenser to improve the rate of condensation in the still.

These modifications are discussed in Section 6.2, which details the reasoning behind the changes made and puts forth a CAD model with these additions for easy visualisation and future reference.

6.2 Improved design

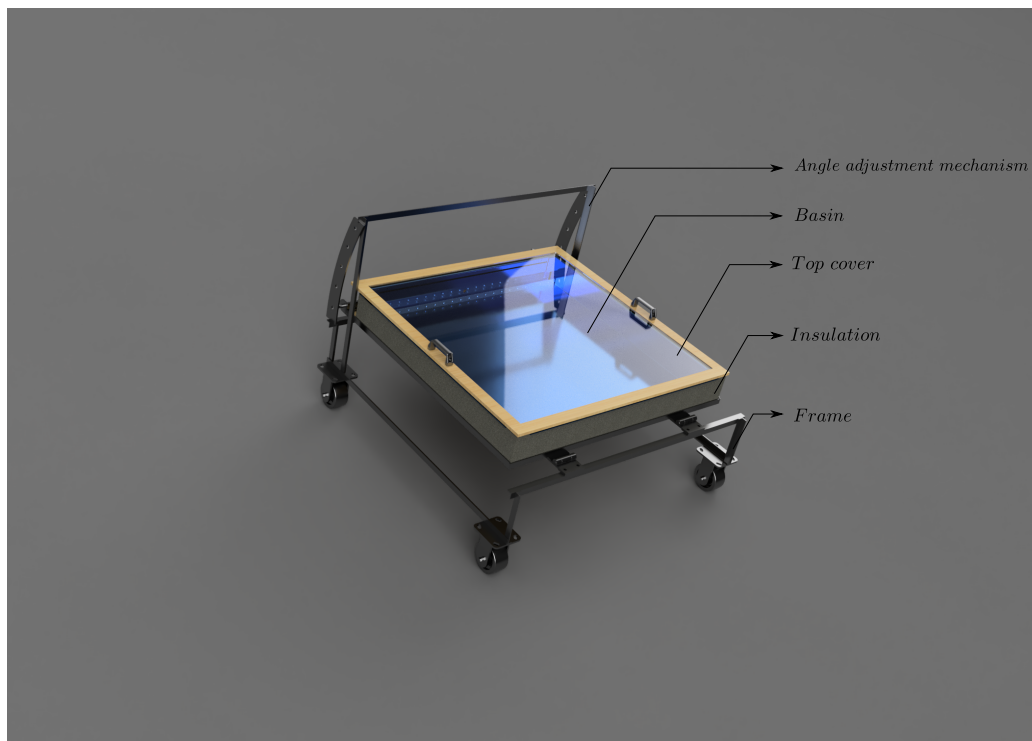


Figure 6.1: A render of the improved model of the still with modifications made to enhance the performance.

The changes that can be made to improve the performance of the still include the addition of a condenser to augment water condensation and a reflector to increase the incident solar energy. However, these are only changes made to the basin of the solar

still. Some modifications can be made to the frame that supports the basin as well, as shown in Fig. 6.1, and discussed subsequently.

These include the addition of an angle adjustment mechanism that allows for modifying the angle of inclination of the still. This would enable the user to adjust the angle of the basin according to the changing seasons, this would improve the year-round performance for the still, as shown in [11].

Changes can also be made to improve the user experience of the solar still. One of these has been discussed in Section 6.2.3, where wheels have been added to the frame of the still. This would enable the user to move the still from one place to another, which can be useful in moving the still from the manufacturing location to the user location, or if external causes necessitate relocation of the solar still.

6.2.1 Adjustable basin inclination

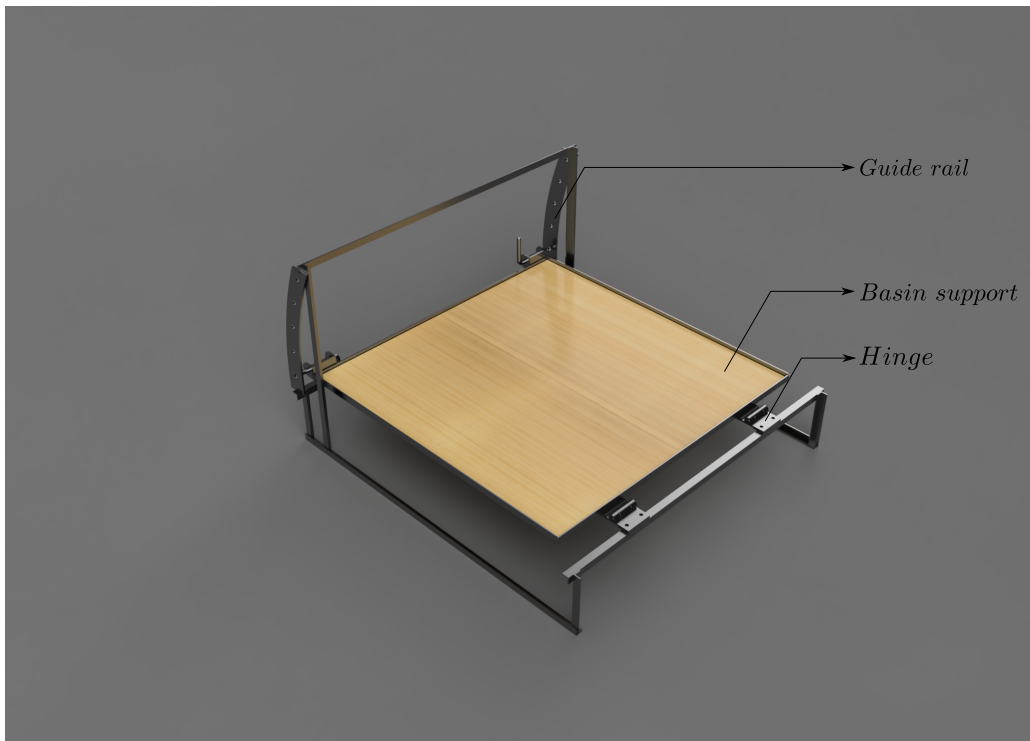


Figure 6.2: A render showing the supporting frame for the basin.

The position of the sun in the sky varies with the seasons, and it has been shown by [15] that changing the still angle improves the performance of the still. To enable this variation, a height adjustment mechanism is shown in Fig. 6.2.

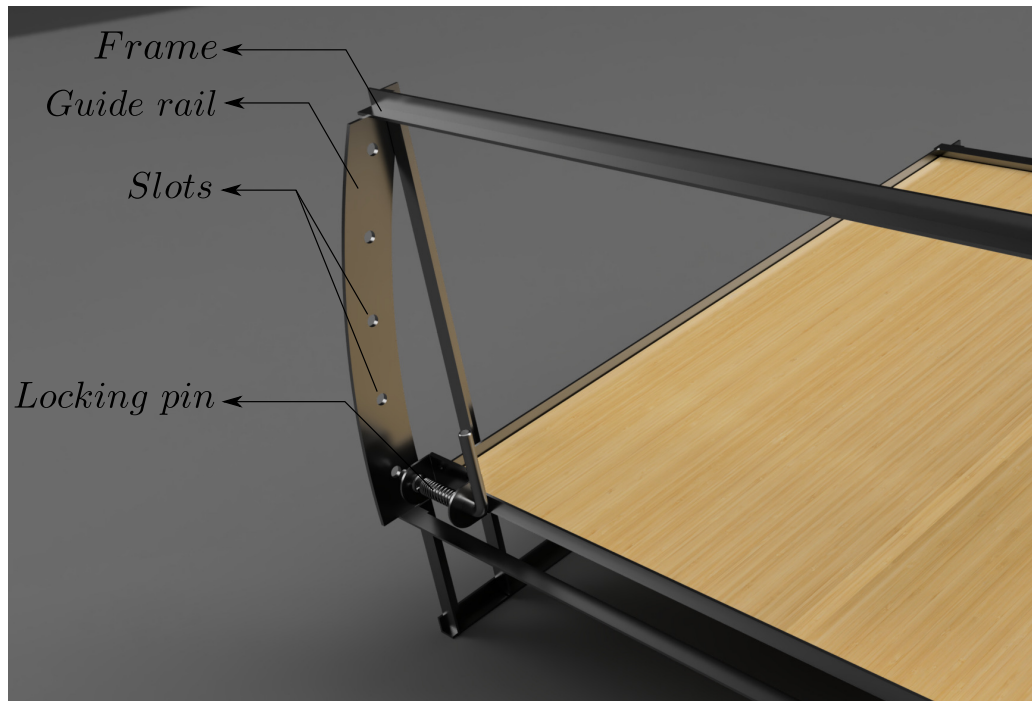


Figure 6.3: A render showing the proposed angle adjustment mechanism.

A closer look at the mechanism is provided by Fig. 6.3. The rails attached to the side of the frame have pre-calibrated attachment slots, which the pins on the basin can slide into to lock the basin at a particular angle. The rails can be modified according to the region for which the still is being developed.

6.2.2 Reflective cover for increasing solar energy input

The amount of solar energy entering the basin directly impacts the performance of the still, hence is a crucial factor that can be influenced by modifications made to the design of the still. A straightforward method to achieve this is to attach a reflective cover to the top of the basin, as shown in Fig. 6.4.

The cover is made out of aluminium sheet metal and is hinged to the frame of the top transparent cover of the basin. This enables the sheet to double as a protective layer for the transparent top cover, saving it from external damage when the still is not in use. A handle is attached to the underside of the reflector, as shown in Fig. 6.5, to improve the user experience.

Modifications were made to the existing prototype to observe the effects of this addition, as shown in Fig. 6.6. An aluminium foil was attached to a skeleton frame

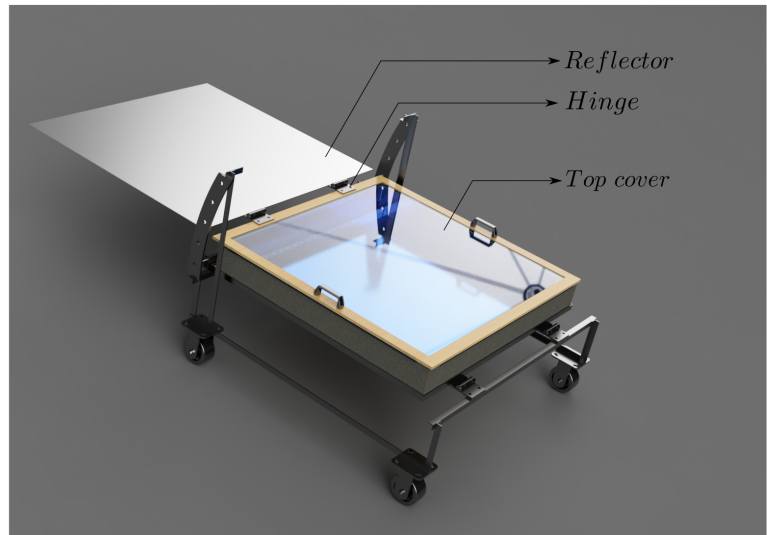


Figure 6.4: A render showing the still model with the reflector attached.

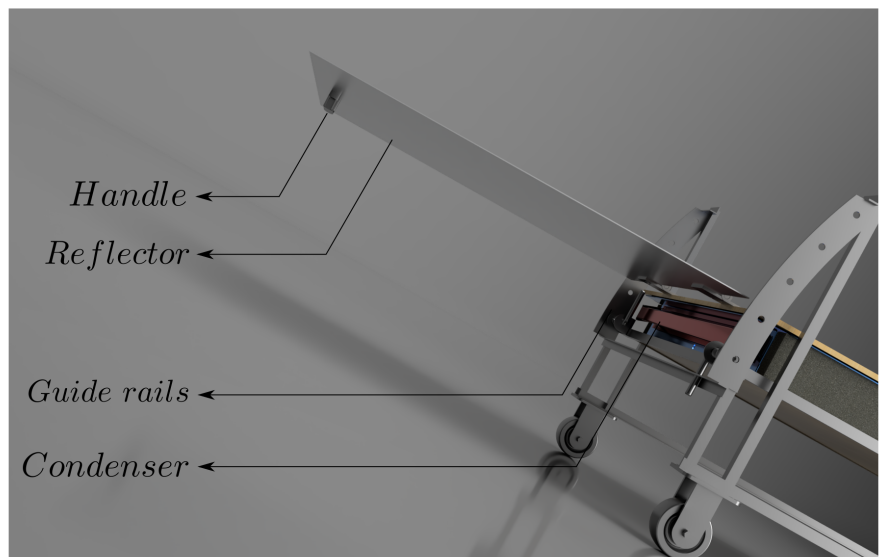


Figure 6.5: A render showing the handle fixed to the reflective cover.

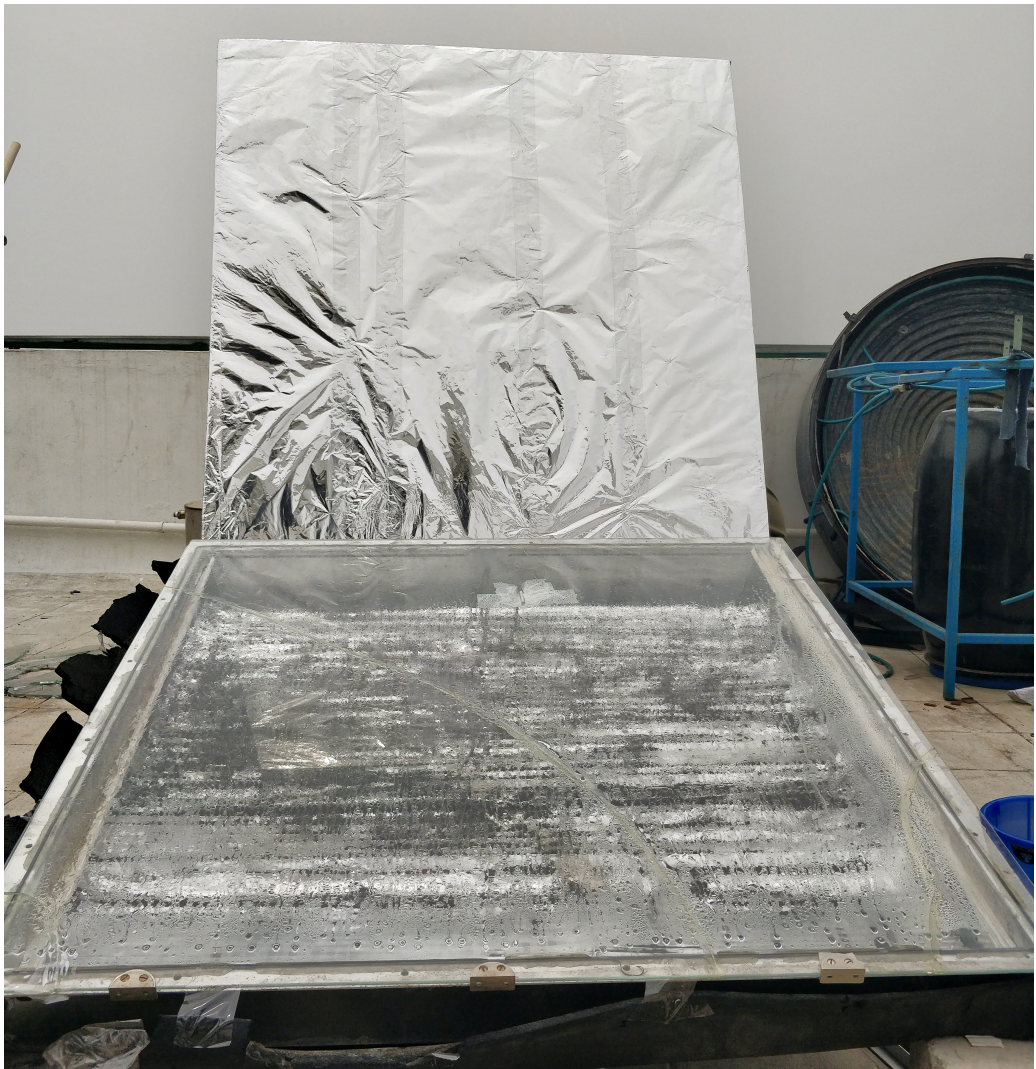


Figure 6.6: A reflective aluminium sheet attached to the still to increase the input solar energy to the still.

made out of polystyrene and aluminium sheet metal, and the angle of the cover was fixed such that the incident sunlight on the basin was maximised.

6.2.3 Movable frame and basin

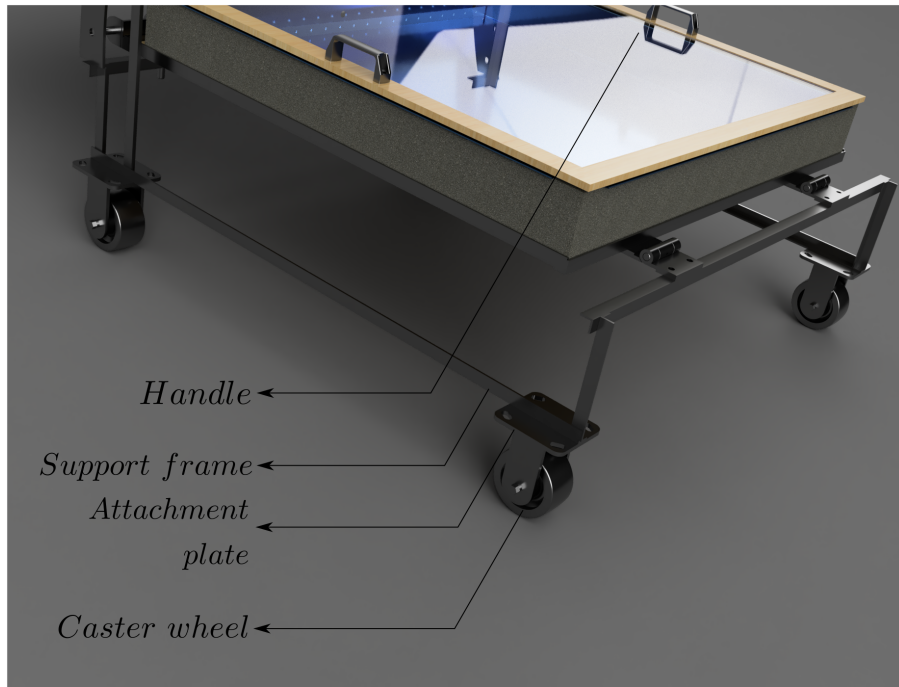


Figure 6.7: A render showing the wheels attached to the frame and the handles on the basin allowing for easy movement.

Providing mobility to the still is advantageous in multiple ways; it allows the user to install the still in an optimal location and orientation with minimal manual effort. It also enables the user to move the still and reorient it if the need arises without much struggle.

The addition of caster wheels to the model is shown in Fig. 6.7; the CAD model of the wheel is sourced from McMaster Carr, an online supplier of parts globally. Handles on the basin allow the user to grip the still firmly while moving the still.

6.3 Future work

Though the benefits of an inclined-basin solar still have been highlighted in Section 6.1, its comparison against the flat-bottomed still requires further investigation. A more exhaustive comparison can be made with the still prototype in [2] after all the suitable modifications have been made to the inclined basin still.

Fabrication of the model proposed in Section 6.2 should also be undertaken, as the addition of an adjustable frame can ease the experimentation and also provide more avenues for investigation, such as varying the basin angle and the reflector angle to find the optimal balance.

The design proposed in Section 6.2 should also be iterated from a DFMA perspective so that the still can be pilot-tested at small scales in various locations with different ambient conditions.

APPENDIX A

The CAD drawings of the first prototype

A.1 Basin sheet metal bending drawing

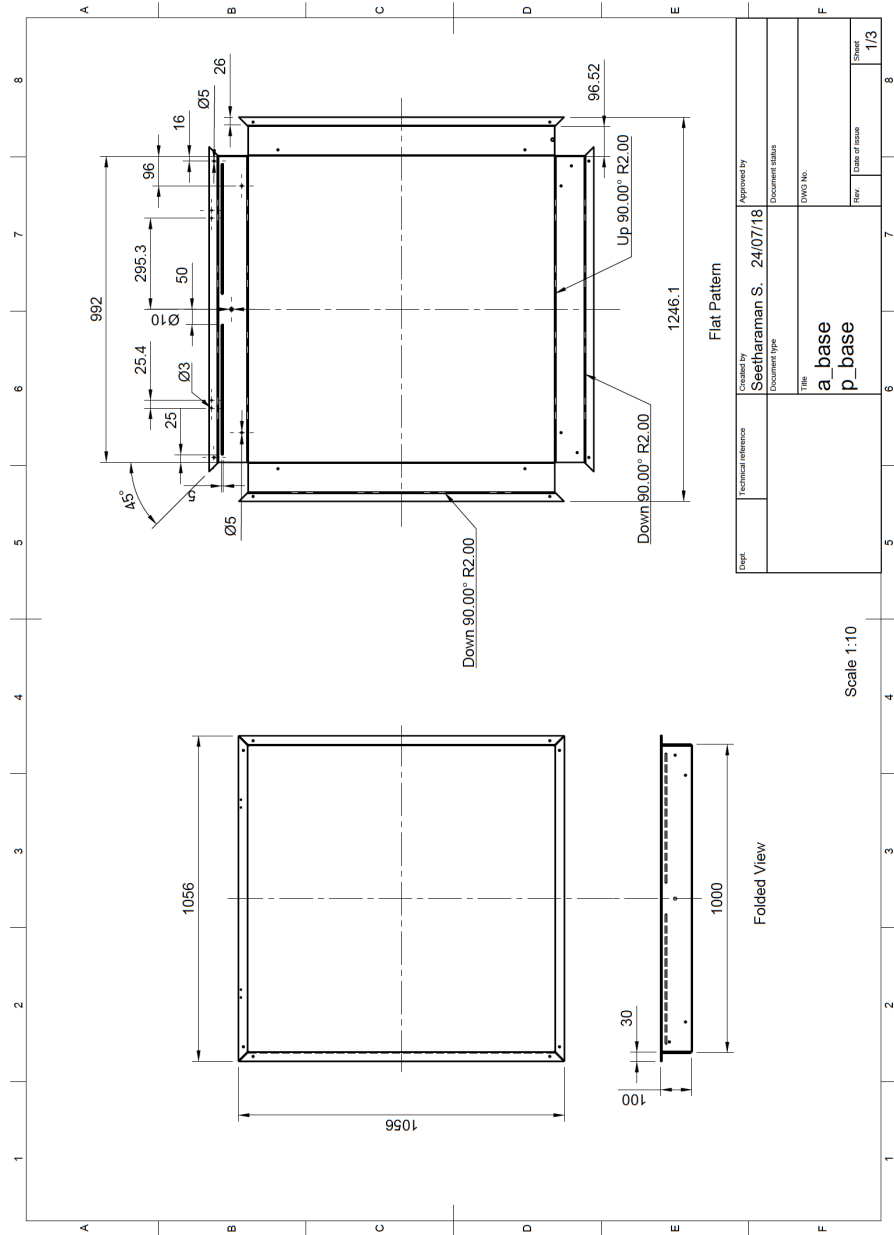


Figure A.1: The 2D CAD drawing of the basin for the first prototype.

APPENDIX B

The CAD drawings of the second prototype

B.1 Basin sheet metal bending drawing

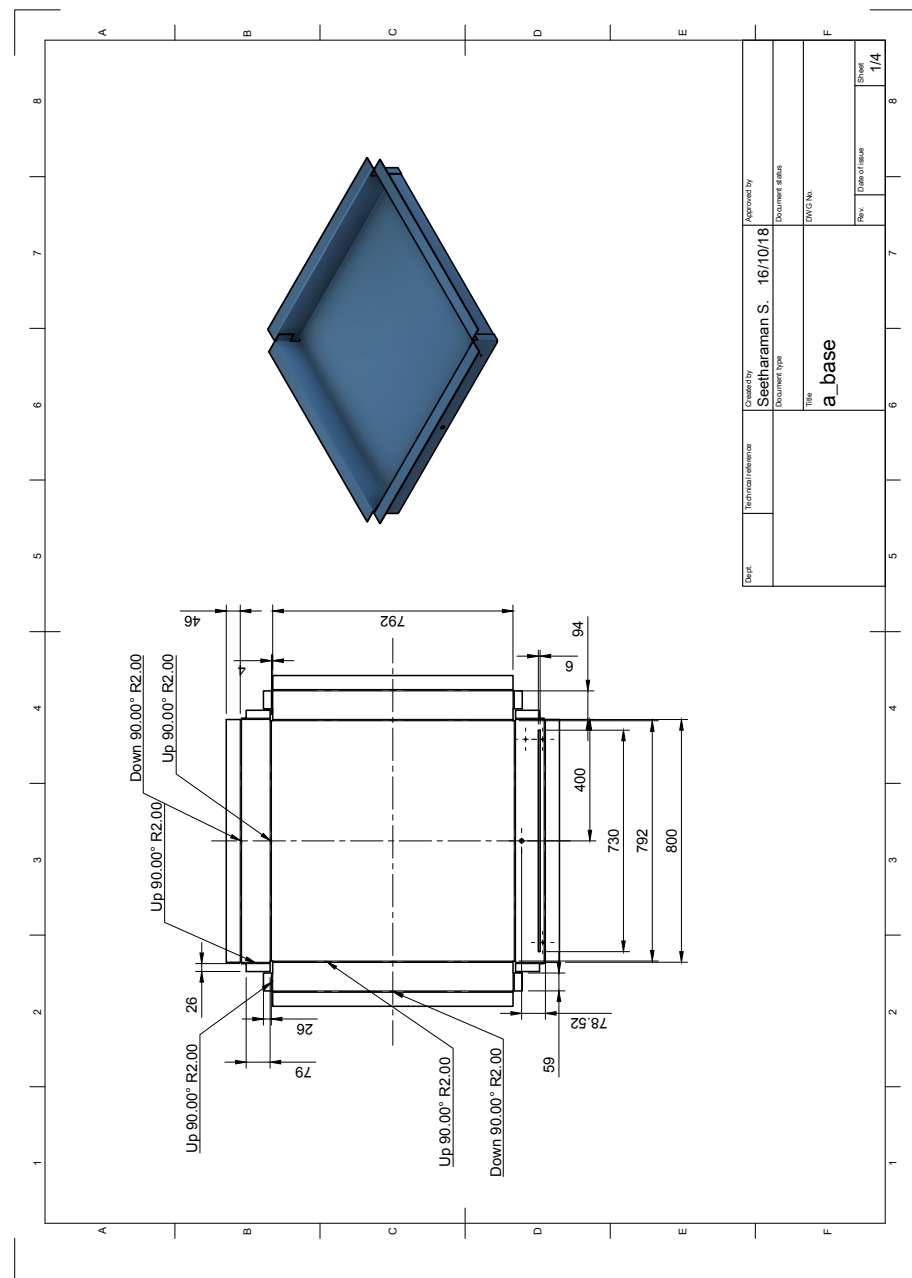


Figure B.1: The 2D CAD drawing of the basin for the second prototype.

REFERENCES

- [1] Food and A. O. of the United Nations, “Thermal insulation materials, technical characteristics and selection criteria,” pp. 1–12, 2015, [Accessed on 2019-05-04]. [Online]. Available: <http://www.fao.org/3/y5013e/y5013e08.htm>
- [2] A. M. Pednekar, S. Bandyopadhyay, and D. Chatterjee, “Performance Evaluation of Solar Still,” in *Proceedings of the 1st International Conference on Mechanical Engineering*, 2018. [Online]. Available: <https://www.researchgate.net/publication/322397441>
- [3] Maps of India, “Drought Affected Areas in India 2016,” 2017, [Accessed on 2019-04-14]. [Online]. Available: <https://www.mapsofindia.com/maps/india/drought-prone-areas.html>
- [4] B. Jamil and N. Akhtar, “Desalination of Brackish Water using Solar Stills-A Review,” Dec. 2014.
- [5] D. RV, “Solar water distillation, the roof type solar still and a multi effect diffusion still, International developments in heat transfer,” *ASME Proceedings of International Heat Transfer; University of Colorado*, vol. 5, pp. 895–902, 1961.
- [6] P. Cooper, “The maximum efficiency of single-effect solar stills,” *Solar Energy*, vol. 15, no. 3, pp. 205–217, 1973.
- [7] World Health Organisation, “Nutrients in Drinking Water,” Tech. Rep., 2005. [Online]. Available: <https://apps.who.int/iris/handle/10665/43403>
- [8] F. Edition, “Guidelines for drinking-water quality,” *WHO chronicle*, vol. 38, no. 4, pp. 104–8, 2011.
- [9] P. V. Kumar, A. Kumar, O. Prakash, and A. K. Kaviti, “Solar stills system design: A review,” *Renewable and Sustainable Energy Reviews*, vol. 51, pp. 153–181, Nov 2015.
- [10] M. S. S. Abujazar, S. Fatihah, A. Rakmi, and M. Shahrom, “The effects of design parameters on productivity performance of a solar still for seawater desalination: A review,” *Desalination*, vol. 385, pp. 178–193, May 2016.
- [11] S. Sharshir, N. Yang, G. Peng, and A. Kabeel, “Factors affecting solar stills productivity and improvement techniques: A detailed review,” *Applied Thermal Engineering*, vol. 100, pp. 267–284, May 2016.
- [12] Ramya Rajagopalan, “Marine Protected Areas in India,” Tech. Rep. 3, 2008. [Online]. Available: <http://nopr.niscair.res.in/handle/123456789/4271>
- [13] H. Garg and H. Mann, “Effect of climatic, operational and design parameters on the year round performance of single-sloped and double-sloped solar still under indian arid zone conditions,” *Solar Energy*, vol. 18, no. 2, pp. 159–163, 1976.

- [14] J. Riera, J. Martínez-Lozano, F. Tejerina, and F. Tena-Sanguesa, “Efficiency of a Solar Still As a Function of Its Main Parameters. Production Estimation for Valencia, Spain,” in *Solar Energy International Progress*. Elsevier, 2013, pp. 1474–1496.
- [15] A. S. Nafey, M. Abdelkader, A. Abdelmalip, and A. A. Mabrouk, “Parameters affecting solar still productivity,” *Energy Conversion and Management*, vol. 41, no. 16, pp. 1797–1809, Nov 2000.
- [16] I. Al-Hayeka and O. O. Badran, “The effect of using different designs of solar stills on water distillation,” *Desalination*, vol. 169, no. 2, pp. 121–127, 2004.
- [17] K. Tarawneh and S. Muafag, “Effect of Water Depth on the Performance Evaluation of Solar Still,” *Jordan Journal of Mechanical and Industrial Engineering*, vol. 1, no. 1, pp. 23 – 29, 2007.
- [18] D. D. W. Rufuss, S. Iniyian, L. Suganthi, and P. Davies, “Solar stills: A comprehensive review of designs, performance and material advances,” *Renewable and Sustainable Energy Reviews*, vol. 63, pp. 464–496, Sep 2016.
- [19] J. Cotruvo, N. Voutchkov, J. Fawell, P. Payment, D. Cunliffe, and S. Lattemann, *Desalination Technology*. CRC Press, Jun 2010. [Online]. Available: <https://www.taylorfrancis.com/books/9781439828939>
- [20] F. Kozisek, “Health Risk from Drinking Demineralized Water,” *Rolling Revision of the WHO Guidelines for Drinking Water Quality*, 2004.
- [21] World Health Organisation, *Guidelines for drinking-water quality: First addendum to 3rd Edition*, Geneva: WHO, 2006, vol. 1. [Online]. Available: <http://www.ncbi.nlm.nih.gov/pubmed/15806952>
- [22] World Health Organization, “Safe Drinking-water from Desalination,” p. 28, 2011, [Accessed on 2019-04-12]. [Online]. Available: <http://apps.who.int/iris/bitstream/10665/70621/1/WHO{ }HSE{ }WSH{ }11.03{ }eng.pdf>
- [23] Greenspec, “Insulation materials and their thermal properties,” 2018, [Accessed on 2019-04-15]. [Online]. Available: <http://www.greenspec.co.uk/building-design/insulation-materials-thermal-properties/>
- [24] Grusin Mike, “BMP180 Barometric Pressure Sensor,” 2016, [Accessed on 2019-04-15]. [Online]. Available: <https://learn.sparkfun.com/tutorials/bmp180-barometric-pressure-sensor-hookup>
- [25] A. Devices, “TMP36 Datasheet and Product Info | Analog Devices,” [Accessed on 2019-05-06]. [Online]. Available: <https://www.analog.com/en/products/tmp36.html#{product-overview}>
- [26] Dejan Nedelkovski, “DHT11 & DHT22 Sensor Temperature and Humidity Tutorial,” 2016. [Online]. Available: <https://howtomechatronics.com/tutorials/arduino/dht11-dht22-sensors-temperature-and-humidity-tutorial-using-arduino/>
- [27] T. Instruments, “LM35 ±0.5 deg C Temperature Sensor with Analog Output with 30V Capability | TI.com,” 2016, [Accessed on 2019-04-15]. [Online]. Available: <http://www.ti.com/product/LM35/description?keyMatch=lm35{&}tisearch=Search-EN-Everythinghttp://www.ti.com/product/LM35>

- [28] G. Mathers, *The welding of aluminium and its alloys*. CRC Press, 2011.
- [29] Maxim Integrated, “DS18B20 Programmable Resolution 1-Wire Digital Thermometer,” Tech. Rep., 2008.
- [30] E. Toolbox, “Specific Heat of Liquids and Fluids,” 2003, [Accessed on 2019-05-01]. [Online]. Available: <https://www.engineeringtoolbox.com/specific-heat-fluids-d{ }151.html>
- [31] J. S. Galsin, “Specific Heat of Solids,” in *Solid State Physics*, 2003, pp. 149–176, [Accessed on 2019-05-01]. [Online]. Available: <https://www.engineeringtoolbox.com/specific-heat-solids-d{ }154.html>
- [32] “WeiHeng Portable Electronic Scale - 0 to 50kg | Afrimash.com - Nigeria,” [Accessed on 2019-05-01]. [Online]. Available: <https://www.afrimash.com/shop/agricultural-equipment/fish-equipment/portable-electronic-scale-0-to-50kg/>